



# Divergent patterns of recent sea ice cover across the Bering, Chukchi, and Beaufort seas of the Pacific Arctic Region



Karen E. Frey<sup>a,\*</sup>, G.W.K. Moore<sup>b</sup>, Lee W. Cooper<sup>c</sup>, Jacqueline M. Grebmeier<sup>c</sup>

<sup>a</sup> Graduate School of Geography, Clark University, Worcester, MA, USA

<sup>b</sup> Department of Physics, University of Toronto, Toronto, Ontario, Canada

<sup>c</sup> University of Maryland Center for Environmental Science, Solomons, MD, USA

## ARTICLE INFO

### Article history:

Available online 27 May 2015

## ABSTRACT

Over the past three decades of the observed satellite record, there have been significant changes in sea ice cover across the Bering, Chukchi, and Beaufort seas of the Pacific Arctic Region (PAR). Satellite data reveal that patterns in sea ice cover have been spatially heterogeneous, with significant declines in the Chukchi and Beaufort seas, yet more complex multi-year variability in the Bering Sea south of St. Lawrence Island. These patterns in the Chukchi and Beaufort seas have intensified since 2000, indicating a regime shift in sea ice cover across the northern portion of the PAR. In particular, satellite data over 1979–2012 reveal localized decreases in sea ice presence of up to  $-1.64$  days/year (Canada Basin) and  $-1.24$  days/year (Beaufort Sea), which accelerated to up to  $-6.57$  days/year (Canada Basin) and  $-12.84$  days/year (Beaufort Sea) over the 2000–2012 time period. In contrast, sea ice in the Bering Sea shows more complex multi-year variability with localized increases in sea ice presence of up to  $+8.41$  days/year since 2000. The observed increases in sea ice cover since 2000 in the southern Bering Sea shelf region are observed in wintertime, whereas sea ice losses in the Canada Basin and Beaufort Sea have occurred during summer. We further compare sea ice variability across the region with the National Centers for Environmental Prediction (NCEP) North American Regional Reanalysis (NARR) wind and air temperature fields to determine the extent to which this recent variability is driven by thermal vs. wind-driven processes. Results suggest that for these localized areas that are experiencing the most rapid shifts in sea ice cover, those in the Beaufort Sea are primarily wind driven, those offshore in the Canada Basin are primarily thermally driven, and those in the Bering Sea are influenced by elements of both. Sea ice variability (and its drivers) across the PAR provides critical insight into the forcing effects of recent shifts in climate and its likely ultimate profound impacts on ecosystem productivity across all trophic levels.

© 2015 Elsevier Ltd. All rights reserved.

## 1. Introduction

The Arctic Ocean has experienced significant warming (Zhang, 2005; Polyakov et al., 2007; Steele et al., 2008) and dramatic declines in sea ice cover (Comiso et al., 2008; Stroeve et al., 2008, 2012; Cavalieri and Parkinson, 2012) over the past few decades. These reductions in sea ice have facilitated positive feedbacks through decreased albedo and enhanced absorption of solar insolation (e.g., Perovich et al., 2007, 2008, 2011), leading to model predictions of a near absence of summer sea ice by the year 2040 (Holland et al., 2006) and possibly sooner (Stroeve et al., 2007; Wang and Overland, 2009, 2012; Overland and Wang, 2013). Changes associated with these declines in sea ice extent include long-term thinning trends

of sea ice (Kwok and Rothrock, 2009; Kwok et al., 2009; Laxon et al., 2003), a lengthening of the summer melt season (Markus et al., 2009), and a shift from primarily perennial multiyear ice to seasonal first-year ice (Maslanik et al., 2007, 2011). These changes have been spurred in part by increased seawater heat fluxes entering the Chukchi Sea through Bering Strait (Shimada et al., 2006; Woodgate et al., 2006; Mizobata et al., 2010), leading to ocean warming that in turn delays autumn sea ice re-growth (Steele et al., 2008). From an atmospheric perspective, these additional heat fluxes may also be associated with Arctic dipole anomalies that have increased poleward wind forcing in the Bering Strait region over the past decade (Wu et al., 2006; Wang et al., 2009, 2014; Overland et al., 2012). Additional modes of climate variability, such as the Arctic Oscillation (AO; Wang and Ikeda, 2000; Rigor et al., 2002; Liu et al., 2004; Stroeve et al., 2011) and the Pacific Decadal Oscillation (PDO; Zhang et al., 2010; Danielson et al., 2011; Wendler et al., 2014), have also been implicated as drivers of sea

\* Corresponding author at: Graduate School of Geography, Clark University, 950 Main Street, Worcester, MA 01610, USA. Tel.: +1 508 793 7209.

E-mail address: [kfrey@clarku.edu](mailto:kfrey@clarku.edu) (K.E. Frey).

ice variability over longer decadal time periods. Overall, observed reductions in sea ice cover across the Arctic have been most pronounced in the marginal seas of the Alaskan and Russian continental shelves (Steele et al., 2008; Stroeve et al., 2012), including the Chukchi and Beaufort seas of the Pacific Arctic Region (PAR).

The PAR includes some of the most seasonally productive marine ecosystems in the world (Grebmeier, 2012) and shifts in sea ice across the region are likely to have profound consequences for seasonal phytoplankton production as well as ecosystem productivity across all trophic levels (e.g., Jin et al., 2009). In particular, the Chukchi Sea (and Canada Basin to the northeast) has experienced some of the fastest declines in sea ice cover across the Arctic (Parkinson and Cavalieri, 2008; Cavalieri and Parkinson, 2012), where the ice-albedo effect plays a significant role in explaining these drastic reductions (Perovich et al., 2007, 2008, 2011; Perovich, 2011). Furthermore, predictions of future sea ice conditions in the Chukchi and Beaufort seas (north of 70°N), show that annual open-water durations may shift from 3 to 4 months currently to nearly 5 months by 2040 (Wang and Overland, 2015).

In the Beaufort Sea, recent sea ice studies have related sea ice distributions to the strength of the Beaufort Gyre (Barber and Hanesiak, 2004; Kwok and Cunningham, 2012; Hutchings and Rigor, 2012; Yu et al., 2013) and have further highlighted that an increased responsiveness of ice drift to geostrophic winds is consistent with a thinner and weaker seasonal sea ice cover (Kwok et al., 2013). The strengthening of the Beaufort Sea High has been identified (Moore, 2012; Wood et al., 2013, 2015) with easterly wind forcing (Wood et al., 2013), which is a likely result of tropospheric warming and a reduction in atmospheric baroclinicity (Moore, 2012). In contrast to larger pan-Arctic trends, however, regional increases in sea ice during winter have recently been reported for the Bering Sea (e.g., Francis and Hunter, 2007; Wendler et al., 2014), in part owing to a weakening of the Aleutian Low resulting in less warm air from the south being advected into the Bering Sea region (thus favoring northerly winds that promote ice formation). Stabenon et al. (2012a) further described multi-year variability in sea ice cover over the southeastern Bering Sea shelf, oscillating between warm years (e.g., 2001–2005) with less extensive ice (driven by weak, easterly

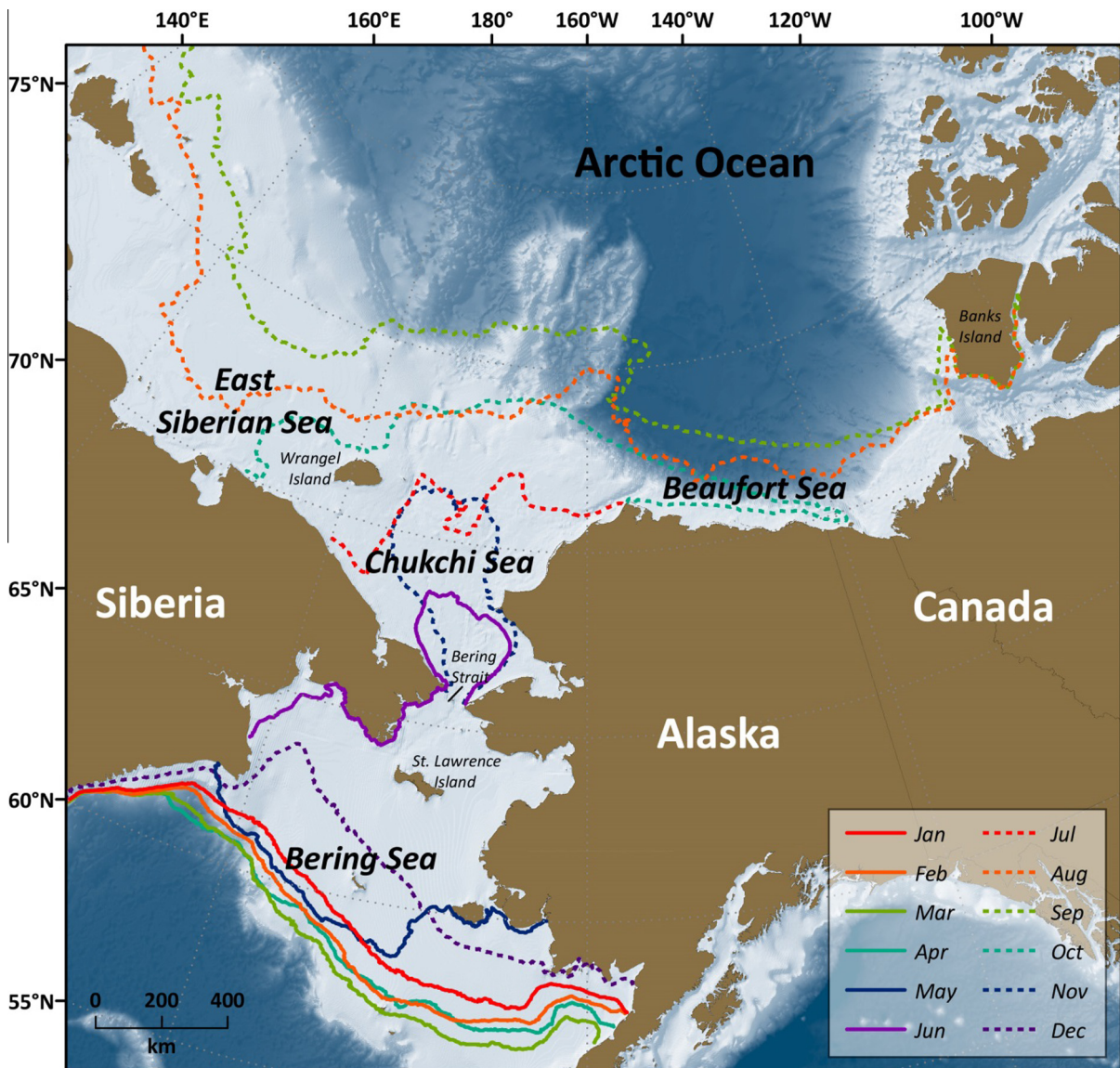


**Fig. 1.** Location of the Pacific Arctic Region, including the East Siberian, Beaufort, Chukchi, and Bering seas. Isolines indicate the mean ice edge (defined using a 15% sea ice concentration threshold) based on AMSR-E satellite data from 2003 to 2011 (January–September) and 2003 to 2010 (October–December). Bathymetry is included for reference. Landfast ice forms along the Beaufort coast before areas farther north offshore in the Beaufort Sea, which is apparent in the ice edge isoline for October.

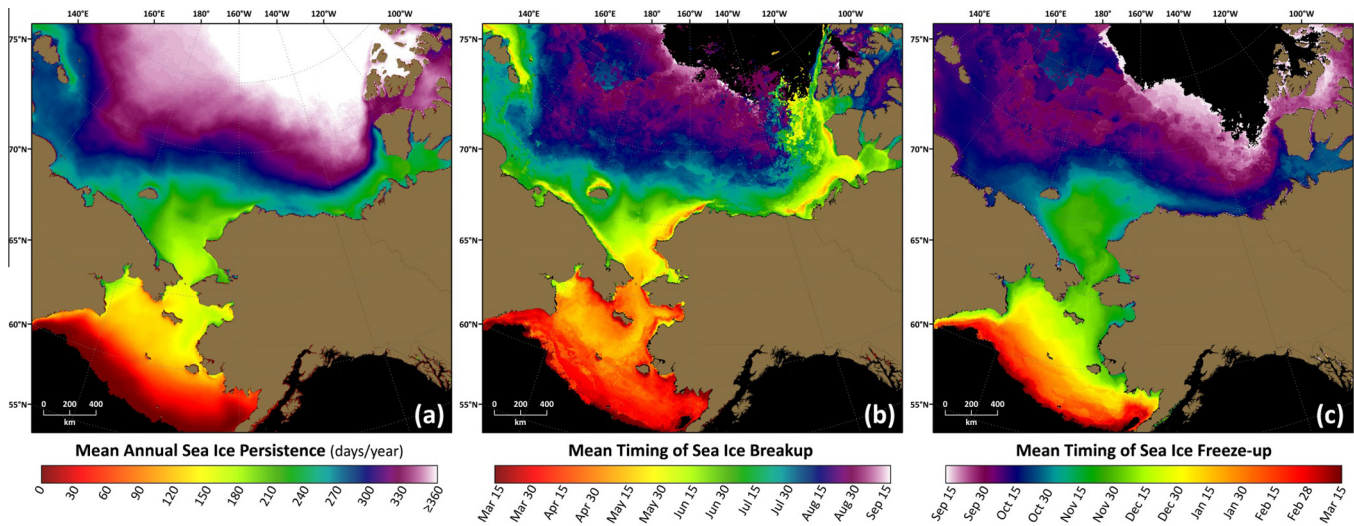


**Fig. 2.** (a) Mean annual sea ice persistence (2003–2010); (b) mean timing of sea ice breakup (2003–2011); and (c) mean timing of sea ice freeze-up (2002/2003–2010/2011) across the Pacific Arctic Region. Values are based on a 15% sea ice concentration threshold using AMSR-E satellite time series.

winds) and cold years (e.g., 2007–2010) with more extensive ice (driven by cold, northerly winds). Stabeno et al. (2012b) described sea ice variability across the southeastern Bering Sea shelf from a spatial perspective as well, where a “decoupling” of patterns of sea ice variability has occurred between the recent summer sea ice minima north in the Arctic (including the Chukchi and Beaufort seas) and subsequent winter/spring sea ice maxima in the southern Bering Sea shelf region.

In this study, we summarize the recent variability in sea ice cover across the broader PAR, including the Bering, Chukchi, and Beaufort seas (Fig. 1). We pay particular attention to sea ice using relatively high spatial resolution (6.25 km) sea ice concentrations derived from the Advanced Microwave Scanning Radiometer for EOS (AMSR-E) sensor on the Aqua satellite platform (Spren et al., 2008). Based on a 15% sea ice concentration threshold to categorize sea ice as being either present or absent, annual sea ice persistence, the timing of sea ice breakup, and the timing of sea ice formation are quantified with AMSR-E data spanning 2003–2011 (up until the point of instrument failure in October 2011). We additionally give the AMSR-E time series context within a longer time frame by using the lower spatial resolution (25 km) sea ice concentration data (spanning the years 1979–2012) derived from the Scanning Multichannel Microwave Radiometer (SMMR) and Special Sensor Microwave/Imager (SSM/I) passive microwave instruments (Cavaliere et al., 2008). We compare sea ice variability across the PAR with National Centers for Environmental Prediction (NCEP) North American Regional Reanalysis (NARR) 10 m wind and 2 m air temperature fields to determine the extent to which recent sea ice variability has been driven by thermal vs. wind-driven processes. In particular, we partition winds in a novel way (winter northwesterly 10 m winds and summer northeasterly 10 m winds), which appears to maximize our understanding of seasonal sea ice persistence across the region. Lastly, we compare sea ice variability across the region with both PDO and AO indices to investigate the extent to which these modes of climate variability affect sea ice cover across the Bering, Chukchi, and Beaufort seas of the PAR.

## 2. Data and methods

The primary methodology for this study is an assessment of recent sea ice conditions throughout the PAR using sea ice

concentrations from the AMSR-E sensor. These data were obtained from the University of Bremen (<http://www.iup.uni-bremen.de/seaice/amsr/>) and use the Arctic Radiation and Turbulence Interaction Study (ARTIST) sea ice algorithm to calculate sea ice concentrations from passive microwave brightness temperatures (Spren et al., 2008). These data (available from June 2002 through October 2011) provide a relatively high spatial resolution (6.25 km) daily time series of sea ice concentrations throughout the PAR. Because of the failure of the AMSR-E sensor in October 2011, it is a timely opportunity to assess the entire time series for spatial and interannual variability in the annual persistence of sea ice cover, as well as the timing of sea ice breakup and formation. Although the time series began in June 2002, we initiated our focus in 2003 (the first full year of data). As is standard in many prior studies, we used a 15% ice concentration threshold to define the presence vs. absence of sea ice cover for calculations of sea ice extent. We then summed the number of days when sea ice was present (for each pixel) within a given year, which resulted in maps of annual sea ice persistence over the years 2003–2010 (those years with complete data available). The timing of sea ice breakup (formation) was determined by flagging the date on which a pixel registered two consecutive days below (above) a 15% sea ice concentration threshold, where we defined the breakup period as March 15–September 15 and the freeze-up period as September 15–March 15. Requiring two consecutive days of the breakup/freezing condition ensured that the defined events were persistent rather than spurious occurrences. We additionally investigated seasonal sea ice persistence over the winter (January, February, March; JFM), spring (April, May, June; AMJ), summer (July, August, September; JAS), and autumn (October, November, December; OND) time periods. Given data availability, the winter, spring, and summer time series span 2003–2011, whereas the autumn time series spans the 2003–2010 time period. Owing to the relatively short time series available for the AMSR-E data, we utilized a Theil-Sen median slope estimator (Sen, 1968) to assess the significance of trends in annual and seasonal sea ice persistence across the region. The Theil-Sen trend uses a robust non-parametric trend operator that is particularly well suited for assessing the rate of change in short and/or noisy time series (Hoaglin et al., 2000). The statistical significance of the Theil-Sen trends ( $p < 0.1$ ) was established using the nonparametric Mann-Kendall test for monotonic trend (Mann, 1945; Kendall, 1975). Three  $75 \times 75$  km sites in the Bering Sea (BRS), Beaufort Sea

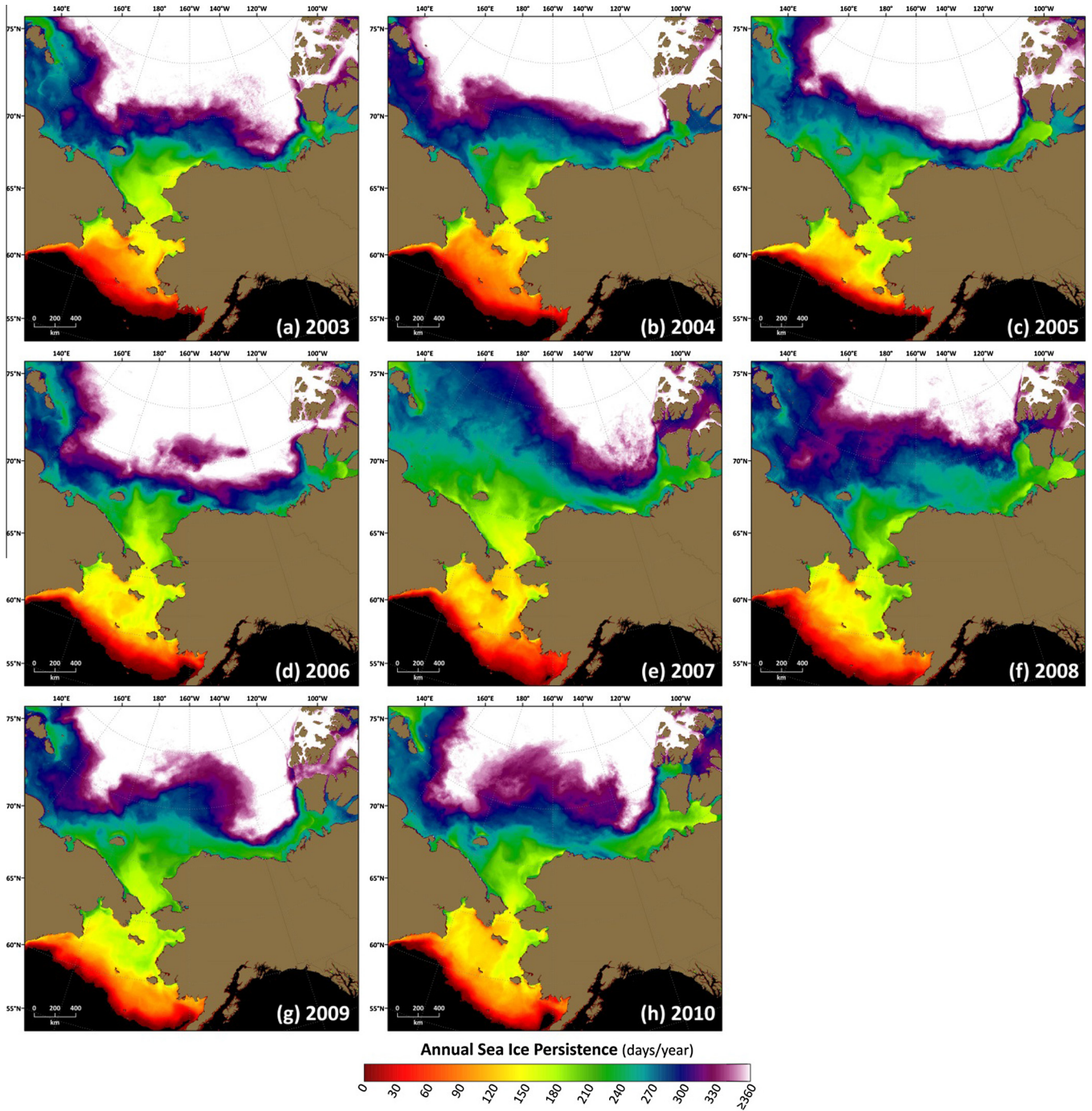


**Fig. 3.** Annual sea ice persistence for the eight full years of the AMSR-E record (2003–2010). Persistence values are based on a 15% sea ice concentration threshold.

(BFS), and Canada Basin (CBS) were identified as sites with notably large shifts in sea ice persistence and were the focus of additional specific statistical investigations. We should note that these sites are not intended to represent the entire region, but rather to serve as focused sites within three distinctly different regions of relatively high trends in sea ice persistence over the time periods investigated.

In order to contextualize more recent AMSR-E based trends in sea ice cover throughout the PAR over a longer time period, sea ice concentrations (spanning the years 1979–2012) derived from SMMR and SSM/I passive microwave instruments (Cavaliere et al., 2008) were also explored in this study. These data (derived with

the NASA Team Algorithm) are available at a 25 km spatial resolution, where the SSM/I data are daily and the SMMR data are available every other day (but were temporally interpolated in this study to create a daily time series). As with the AMSR-E sea ice dataset, we used a 15% ice concentration threshold to define the presence vs. absence of sea ice cover for each pixel in the resulting daily time series. We then summed the number of days when sea ice was present (for each pixel) within a given year, which resulted in maps of annual sea ice persistence over the years 1979–2012. Because these time periods were sufficiently long, ordinary least squares regressions were then mapped spatially (for each pixel) over the 1979–2012 and 2000–2012 time periods, where the slope

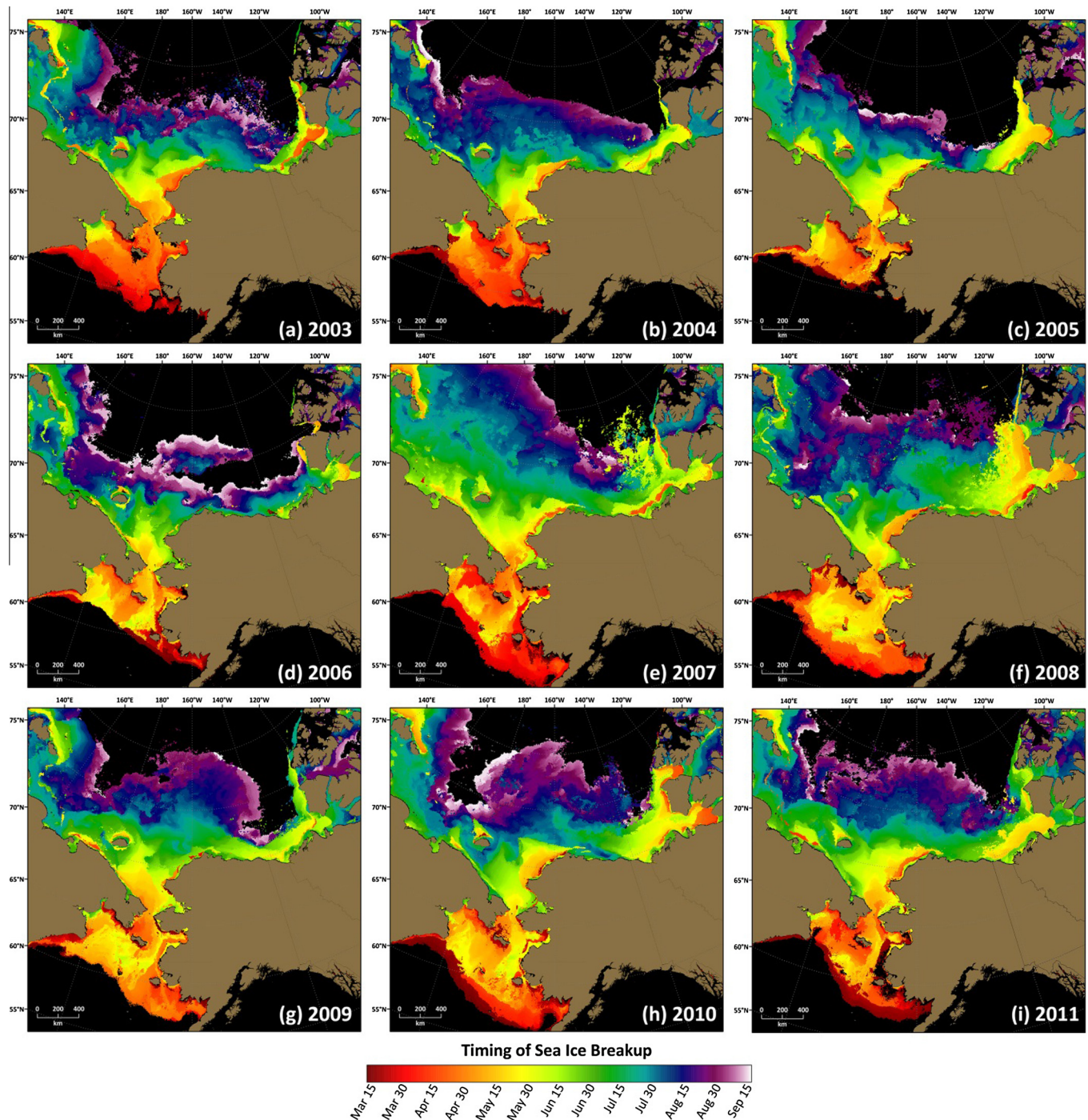


**Fig. 4.** The timing of sea ice breakup for each available year of the AMSR-E record (2003–2011). The timing calculated requires that a pixel register two consecutive days below a 15% sea ice concentration threshold. Black areas to the south denote areas of open water that were not ice covered during the year; black areas to the north denote areas of multiyear ice that did not break up during the year.

coefficients of the regressions denote a change in annual sea ice persistence (days/year). As with the AMSR-E time series, the statistical significance of the SMMR- and SSM/I-based trends ( $p < 0.1$ ) was established using the Mann–Kendall test for monotonic trend.

The long-term (1979–present) NCEP NARR dataset was developed to provide a higher spatial resolution and more accurate climate reanalysis at the continental scale as compared to previous global reanalysis datasets (Mesinger et al., 2006). We utilized both the 2 m surface air temperature ( $T_{2m}$ ) and near-surface 10 m wind fields at a native 32 km horizontal spatial resolution (on a polar

stereographic grid). Both the temperature and wind data were separated into seasonal components, where particular focus was given to winter (JFM) and summer (JAS) time periods when the steepest trends in sea ice were observed. To provide further insight into sea ice variability across the region, we partitioned the wind field into both winter northwesterly (NW) 10 m winds and summer northeasterly (NE) 10 m winds. These seasonal wind fields were then calculated as the occurrence frequency (%) of NW and NE winds during winter and summer, respectively. Linear trends (calculated through ordinary least squares regressions) of the occurrence

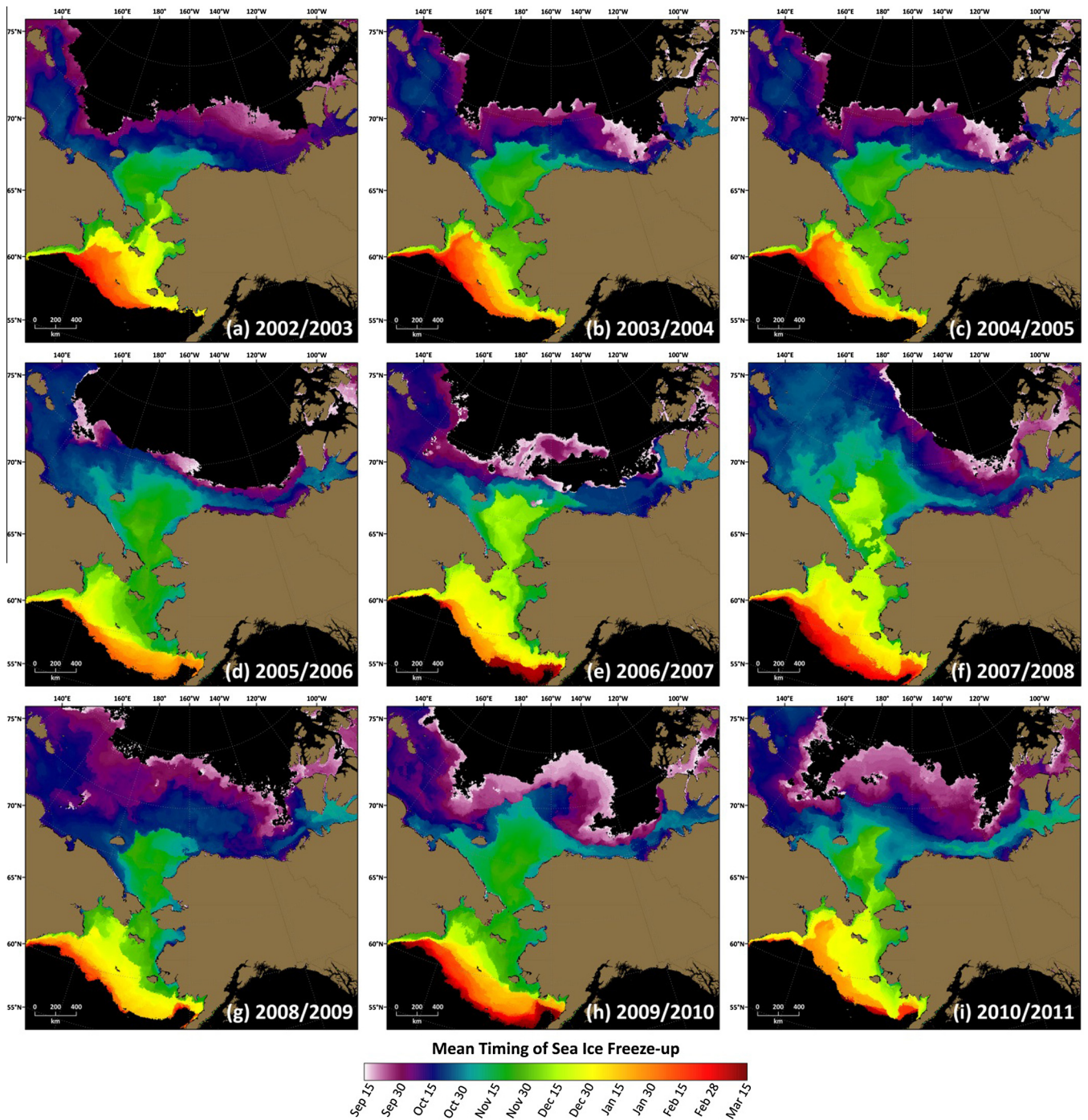


**Fig. 5.** The timing of sea ice freeze-up for each available year of the AMSR-E record (2002/2003–2010/2011). The timing calculated requires that a pixel register two consecutive days above a 15% sea ice concentration threshold. Black areas to the south denote areas of open water that were not ice covered during the year; black areas to the north denote areas of multiyear ice that did not re-freeze during the year. Relatively early freeze-up dates along the Beaufort and Chukchi coastlines are indicative of landfast ice forming here before areas farther north offshore in the Beaufort and Chukchi seas.

frequency of these partitioned winds were calculated spatially for both the 1979–2012 and 2000–2012 time periods. Spatial correlations between reanalysis data (partitioned winds and  $T_{2m}$ ) and AMSR-E derived seasonal sea ice persistence (2003–2011) were additionally performed to provide insight into the potential specific drivers of recent sea ice variability. All time series were first detrended (to force stationarity) before correlation coefficients were calculated. Finally, mean winter (JFM) and summer (JAS)

AO climate indices (from the Climate Prediction Center at NOAA, <http://www.cpc.ncep.noaa.gov/>) and PDO climate indices (from the Joint Institute for the Study of the Atmosphere and Ocean at the University of Washington, <http://jisao.washington.edu/pdo/>) were spatially correlated with SMMR and SSM/I winter and summer seasonal sea ice persistence to provide additional insights into sea ice variability across the region. In this case, the longer-term SMMR and SSM/I time series (1979–2012) was utilized in order

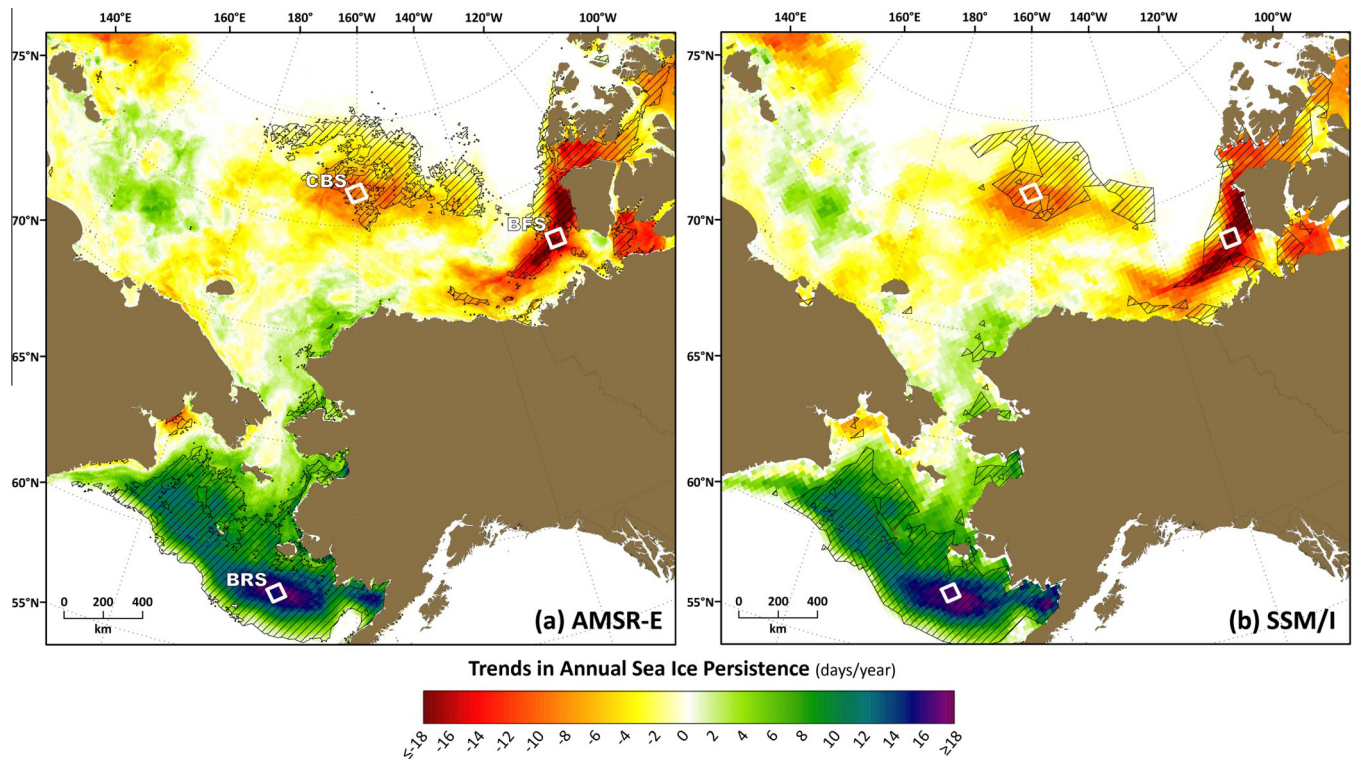


**Fig. 6.** Theil-Sen median trends in annual sea ice persistence (days/year) over the 2003–2010 period for the (a) AMSR-E (6.25-km resolution) and (b) SSM/I (25-km resolution) satellite time series. Hatching indicates statistically significant regions ( $p < 0.1$ ) using the Mann–Kendall test for trend. The three sites demarcated in (a) highlight characteristically steep trends for the Canada Basin (CBS), Beaufort Sea (BFS), and Bering Sea (BRS), the mean time series for which are shown in Fig. 8 (and summarized in Table 1).

**Table 1**  
Trends in annual and seasonal sea ice persistence (days/year) for focused analysis sites in the Canada Basin (CBS), Beaufort Sea (BFS), and Bering Sea (BRS) for both the SMMR, SSM/I time series and the AMSR-E time series. The SMMR, SSM/I values are calculated as (ordinary least squares) linear trends and the AMSR-E values are calculated as Theil-Sen median trends (owing to the shorter time series). Statistical significance of trends is designated as  $p < 0.01$  (bolded/underlined),  $p < 0.05$  (bolded), and  $p < 0.1$  (underlined).

	SMMR, SSM/I Annual (1979–2012)	SMMR, SSM/I Annual (2000–2012)	AMSR-E Annual (2003–2010)	AMSR-E Winter (JFM) (2003–2011)	AMSR-E Spring (AMJ) (2003–2011)	AMSR-E Summer (JAS) (2003–2011)	AMSR-E Autumn (OND) (2003–2010)
Canada Basin Site (CBS)	<u><b>-1.64</b></u>	<u><b>-6.57</b></u>	<b>-9.32</b>	0	0	<b>-6.61</b>	<u><b>-1.23</b></u>
Beaufort Sea Site (BFS)	-1.24	<u><b>-12.84</b></u>	<u><b>-16.07</b></u>	0	-0.11	<b>-8.41</b>	<u><b>-2.51</b></u>
Bering Sea Site (BRS)	0.85	<b>8.41</b>	<u><b>15.55</b></u>	<b>8.61</b>	<u><b>4.12</b></u>	0	0

to foster comparisons over a multi-decadal time period, which would not be possible with the shorter AMSR-E dataset. Again, all climate indices and sea ice image time series were first linearly detrended to force stationarity before correlation analyses were performed.

Ancillary datasets to explore components related to AMSR-E derived sea ice variability across the PAR include monthly sea surface temperature (SST) data (Level 3, 4.6 km spatial resolution) derived from the Moderate Imaging Spectrometer (MODIS) sensor on the Aqua satellite platform obtained from NASA (<http://ocean-color.gsfc.nasa.gov/>) and monthly chlorophyll-*a* concentrations (case I water product, 4.6 km spatial resolution) obtained from the Globcolour Project (<http://www.globcolour.info/>). The Globcolour chlorophyll-*a* concentration dataset maximizes spatial and temporal coverage by combining available data from three satellite sensors (MODIS-Aqua, Medium Resolution Imaging Spectrometer Instrument (MERIS), and Sea-viewing Wide Field of view Sensor (SeaWiFS)).

### 3. Results

Sea ice cover across the PAR is seasonally variable, with much of the Bering, Chukchi, and Beaufort seas covered with first-year sea ice for several months of each year. Northern portions of the Chukchi and Beaufort seas have also contained variable amounts of multiyear sea ice (i.e., ice that has survived at least one melt season) over the last three decades of the observed satellite record. Positions of the monthly mean sea ice edge obtained from the AMSR-E satellite record are shown in Fig. 1. The position of the mean ice edge during winter and early spring (January through April) is farthest south and relatively stable until May when the edge begins to retreat northward. By June, the ice edge on average has retreated northward through the Bering Strait and by September, the ice edge is at its most northern position off the continental shelf in the Chukchi and Beaufort seas. The spatial patterns of sea ice variability can be seen more readily in spatially continuous maps of mean annual sea ice persistence, the timing of sea ice

breakup, and the timing of sea ice freeze-up (Fig. 2). As the PAR includes both first-year and multiyear ice, the annual sea ice persistence throughout the region ranges widely from 0 to 365 days and the most persistent ice is located in the northeastern sector toward the Canadian Archipelago (Fig. 2a). Patterns in the timing of breakup (Fig. 2b) roughly follow latitude, except in cases where winds likely open localized polynyas (e.g., north of Wrangel Island, southwest of Barrow, west of Banks Island, and in the southeastern Beaufort Sea). Sea ice freeze-up occurs in most of the areas off the continental shelf (in the Canada Basin north of the Chukchi and Beaufort seas) by the end of October, by the end of November in the Chukchi Sea, and from December through February/March in the Bering Sea (Fig. 2c). Relatively early freeze-up dates along the Beaufort coast are indicative of landfast ice forming here before areas farther north offshore in the Beaufort Sea. Investigation of individual years of sea ice persistence (Fig. 3), the timing of sea ice breakup (Fig. 4), and the timing of sea ice freeze-up (Fig. 5) also gives important insights into the interannual variability in sea ice over the past decade. In particular, those years with relatively short annual sea ice persistence result from both earlier breakups and later freeze-ups. Furthermore, those areas of highest interannual variability in sea ice cover tend to be those at the southern ice edge in the Bering Sea, at the northern ice edge off the continental shelf in the Canada Basin, and in the region directly west of Banks Island.

Spatial trends in annual sea ice persistence provide a means for identifying those areas registering the most rapid changes. Theil-Sen median trends in annual sea ice persistence over the years 2003–2010 using AMSR-E data are shown in Fig. 6a, where there are two distinct areas of statistically significant ( $p < 0.1$ ) negative trends: significant losses in the Canada Basin north of the Chukchi Sea (−9.32 days/year at the CBS site) and significant losses in the Beaufort Sea west of Banks Island (−16.07 days/year at the BFS site) (Fig. 6a; Table 1). Although these sites were chosen simply

because they highlight notably steep trends in sea ice persistence across the region, the BFS site happens to be in the proximity of the Cape Bathurst polynya. However, as we are focused on reporting overall trends in sea ice persistence, that should not impact the overall metrics used to describe changes in sea ice across this region. The longer-term SMMR and SSM/I data were also used to contextualize the more recent AMSR-E based trends. Theil-Sen median trends in annual sea ice persistence using SSM/I data (over the years 2003–2010; Fig. 6b) show distinctly similar patterns in sea ice changes even with the lower spatial resolution data (25 km vs. 6.25 km), which justifies at least a first-order compatibility between the two datasets. With a longer-term perspective using the SMMR and SSM/I time series (1979–2012), trends in annual sea ice persistence are more subdued, although sea ice losses in the Chukchi Sea, Beaufort Sea, and Canada Basin remain clear (Fig. 7a). These trends clearly accelerated over the 2000–2012 time period (Fig. 7b). For example, satellite data over 1979–2012 reveal localized trends in sea ice cover up to −1.64 days/year (CBS site) and −1.24 days/year (BFS site); these trends accelerated to −6.57 days/year (CBS site) and −12.84 days/year (BFS site) over the 2000–2012 time period (Table 1). A comparison of trends over the SMMR and SSM/I based time series and AMSR-E based time series for these two example CBS and BFS sites illustrate the consistency between the two datasets as well as the acceleration of trends over the past decade (Fig. 8). In contrast, we observe apparent significant gains in sea ice cover over the southern Bering Sea shelf (+15.55 days/year at the BRS site) over the 2003–2010 time period (Figs. 6 and 8c; Table 1), yet this site does not experience a significant trend over the longer 1979–2012 time period (Figs. 7a and 8c; Table 1). It is clear by examining the time series of sea ice cover at the BRS site (Fig. 8c) that this region is experiencing a pattern of multi-year variability of sea ice cover, where 1979–2000 was characterized by high interannual variability in

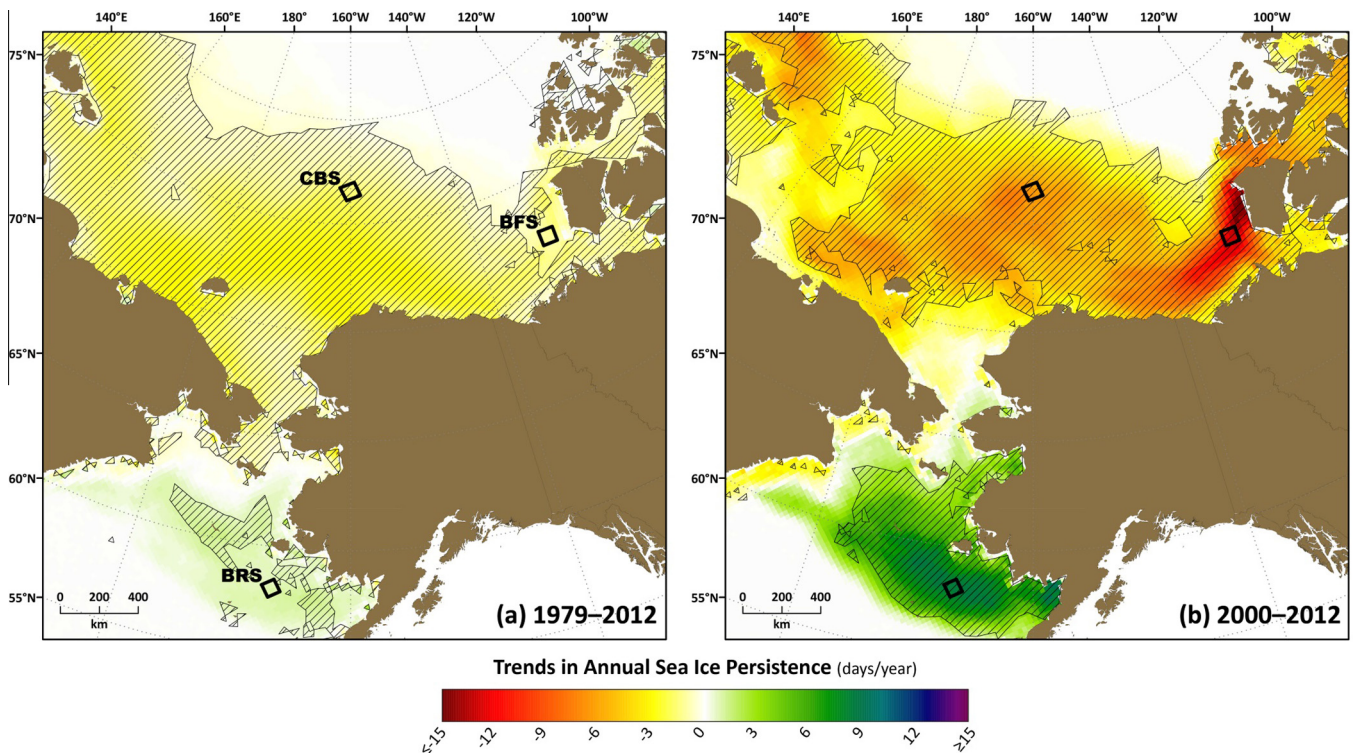


**Fig. 7.** Linear trends in annual sea ice persistence (days/year) based on SMMR and SSM/I sea ice concentrations for (a) 1979–2012 and (b) 2000–2012. Hatching indicates statistically significant regions ( $p < 0.1$ ) using the Mann-Kendall test for trend. Mean time series for representative sites CBS, BFS, and BRS are shown in Fig. 8 (and summarized in Table 1).

sea ice, 2001–2005 was characterized by relatively low sea ice cover, and 2006–2012 was characterized by relatively high sea ice cover. As such, although part of broader multi-year patterns of sea ice variability, this is consistent with the sea ice gains over the last decade across the southern Bering Sea shelf that we (and others) have observed.

Partitioning sea ice persistence by season further elucidates the recent shifts in sea ice over the past decade, where gains in sea ice in the Bering Sea have primarily occurred during winter and losses in sea ice in the Chukchi Sea/Canada Basin and Beaufort Sea have primarily occurred during summer (Fig. 9). It should be noted that although winter sea ice areal coverage may not have observably decreased in the Chukchi Sea/Canada Basin, old and thick multi-year sea ice has significantly declined across the Arctic during winter (as measured in March) since 1980 (e.g., Maslanik et al., 2011). However, as we focus this study on sea ice areal coverage and quantify trends over the decadal AMSR-E time series, we find that the BRS site has gained ice during winter at +8.61 days/year, while the CBS and BFS sites have lost summer ice at –6.61 days/year and –8.41 days/year, respectively (Table 1). The CBS site has additionally lost ice during autumn at a rate of –1.23 days/year, which suggests that freeze-up has shifted to later dates within this region. Statistically significant trends also exist for the BRS site during spring (+4.12 days/year), suggesting that breakup dates have shifted slightly later throughout this region over the past decade (although earlier freeze-up dates account for more of the overall sea ice gains, as indicated by greater rates of sea ice gains during winter months).

During the winter, surface atmospheric circulation in the PAR is dominated by a ridge extending northeast from the Siberian High over the western Arctic and the Aleutian Low (Fig. 10). As a result, there is predominantly northeasterly flow over much of the PAR. During the summer, the Beaufort High is established as a distinct circulation feature (as opposed to being a ridge extending from the Siberian High). Also during the summer, the wintertime Aleutian Low shifts northward and is reduced to a mesoscale feature that extends over the Bering Strait region. As a result, easterly flow persists over the southern Beaufort Sea, westerly flow exists north of the Beaufort Sea, and cyclonic circulation exists over the Bering Sea. Linear trends in the occurrence frequency of NW 10 m winds during the winter (Fig. 11a and b) and NE 10 m winds during the summer (Fig. 11c and d) indicate shifting air circulation patterns across the region, when both the 1979–2012 and 2000–2012 records are considered. These trends show that since 2000, NE flow during summer off Banks Island and NW air flow during the summer over the Bering Sea have become more frequent.

In order to quantify the extent to which recent shifts in sea ice variability can potentially be explained by either thermal or wind-driven processes, spatial correlations between seasonal sea ice persistence and NARR 10 m winds and  $T_{2m}$  were evaluated for both winter and summer (Fig. 12). Given the number of years in the high-resolution time series is 9 (and therefore the degrees of freedom = 7), Pearson correlation coefficients for a two-tailed test are required to be  $|R| \geq 0.582$  for  $p < 0.1$ . Graphically, we use hatching patterns to indicate those correlation coefficients that are statistically significant (Fig. 12). Specific  $R$ -values between sea ice persistence and NARR fields (10 m winds and  $T_{2m}$ ) for the CBS, BFS, and BRS sites are tabulated in Table 2. Significant correlations during winter exist only in the Bering Sea (Fig. 12a and b), where positive correlations are found between the occurrence frequency of NW 10 m winds and sea ice persistence ( $R = 0.83$  for the BRS site) and negative correlations are found between  $T_{2m}$  and sea ice persistence ( $R = -0.91$  for the BRS site). Variance in the summer sea ice persistence in the eastern Beaufort Sea is primarily correlated with NE 10 m winds (Fig. 12c), where  $R = -0.77$  for the BFS site (Table 2). In the western

and central Beaufort Sea slightly offshore, there are statistically significant negative correlations between summer sea ice persistence and  $T_{2m}$ , although these regions have not experienced declines in sea ice cover nearly as drastically as in the eastern Beaufort Sea near the BFS site. For the Canada Basin, the variance in summer sea ice persistence can be explained primarily by summer  $T_{2m}$  (Fig. 12d;  $R = -0.73$  for the CBS site). Although correlations with summer winds at the CBS site were not statistically significant, the broader Canada Basin region shows statistically significant positive correlations with summer NE 10 m winds (Fig. 12c). It should be noted that sea ice persistence during winter at the CBS and BFS sites are constant over time at 90 days, and during summer at the BRS site are constant over time at 0 days. Although this statistically explains why the correlation coefficients for these sites during these seasons compute to 0, it is still meaningful to note that winter winds and summer  $T_{2m}$  in these regions do not have an influence on areal coverage of sea ice, which is the sea ice parameter we are focused on in this study.

We additionally investigated spatial correlations between winter and summer seasonal persistence of sea ice cover with both PDO and AO climate indices to further elucidate how broader climate drivers may be impacting sea ice variability across the PAR (Fig. 13). In this case, the longer-term SMMR and SSM/I time series (1979–2012) was utilized to foster comparisons over a multi-decadal time period, which would not be possible with the shorter AMSR-E dataset. We do not investigate correlations with the Arctic Dipole Anomaly in particular here, as this is likely only a more recent driver of sea ice variability since ~1995 (Wang et al., 2009, 2014). Given the number of years in the

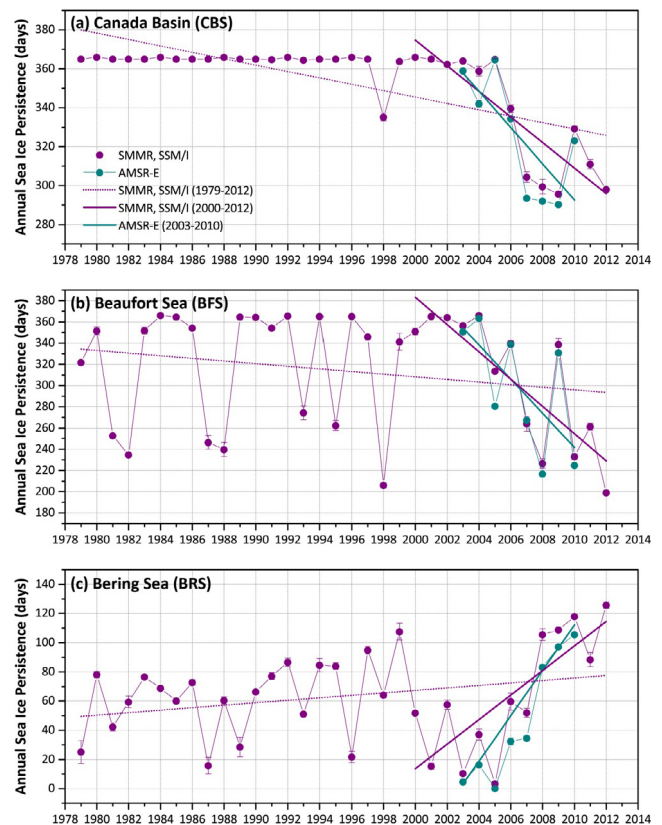


**Fig. 8.** Time series for notable regions with relatively steep trends in annual sea ice persistence for sites in the (a) Canada Basin (CBS); (b) Beaufort Sea (BFS); and (c) Bering Sea (BRS). The locations of sites are shown in Fig. 8. Trend lines are shown for 1979–2012 and 2000–2012 for SMMR and SSM/I data and 2003–2010 for AMSR-E data. Error bars represent the variability ( $\pm 1SD$ ) within the defined  $75 \times 75$  km area boxes. The magnitude and significance of trends are shown in Table 1.

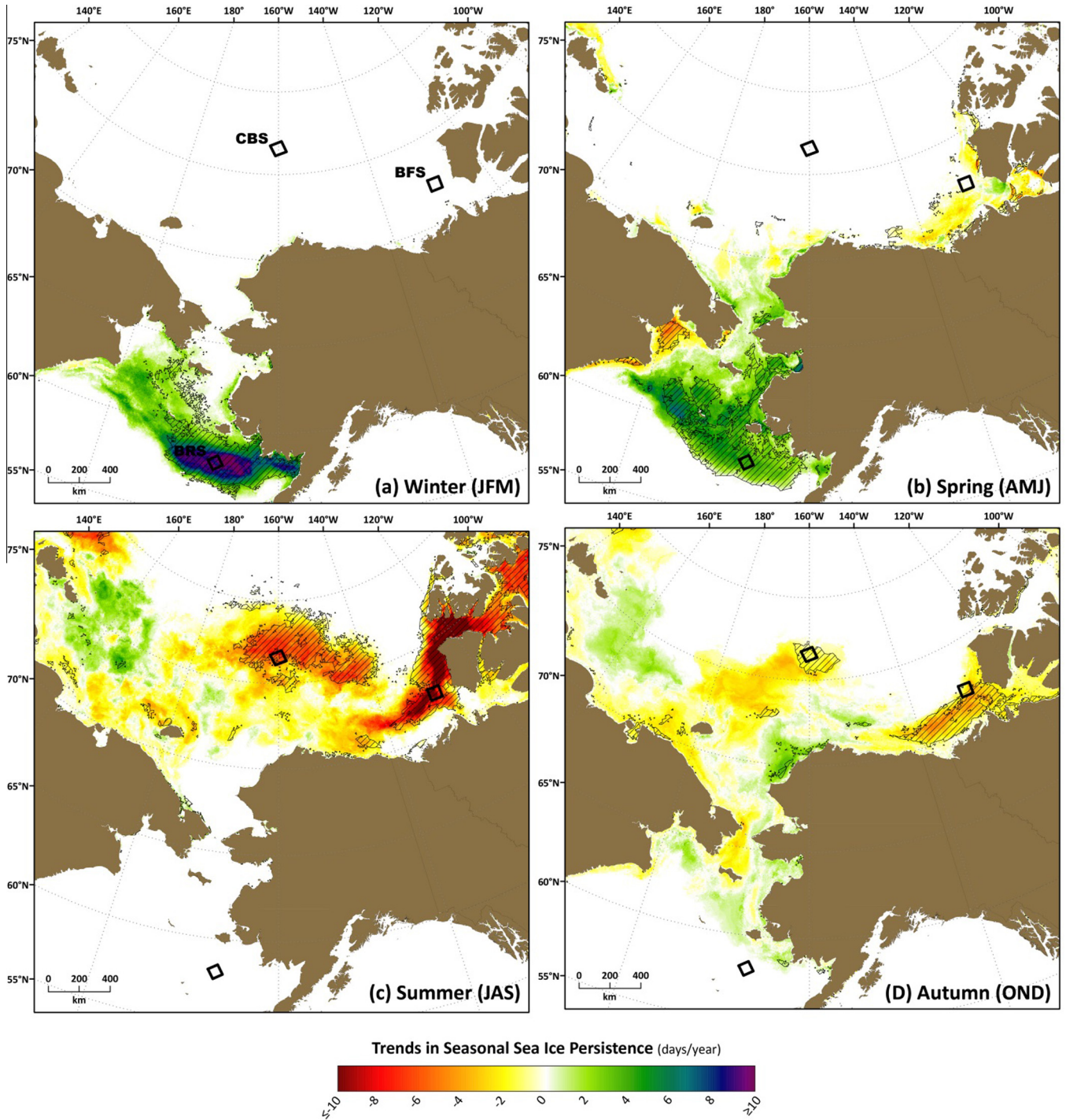


**Fig. 9.** Theil-Sen median trends in seasonal sea ice persistence (days/year) based on available AMSR-E sea ice concentrations for (a) Winter (JFM); (b) Spring (AMJ); (c) Summer (JAS); and (d) Autumn (OND). Hatching indicates statistically significant regions ( $p < 0.1$ ) using the Mann–Kendall test for trend. Winter, Spring, and Summer trends are based on the years 2003–2011; Autumn trends are based on the years 2003–2010. Mean trends for representative sites CBS, BFS, and BRS are summarized in Table 1.

lower-resolution SMMR and SSM/I time series (34, with degrees of freedom = 32), Pearson correlation coefficients for a two-tailed test are required to be  $|R| \geq 0.287$  for  $p < 0.1$ . Again, hatching indicates those correlation coefficients that are statistically significant (Fig. 13). During winter, we find significant negative correlations between sea ice on the southeastern Bering Sea shelf and the PDO (Fig. 13a) as well as significant positive correlations between sea ice slightly farther north (just south of St. Lawrence Island) and

the AO (Fig. 13b). During summer, we observe significant positive correlations between sea ice in the Canada Basin/Canadian Archipelago and the PDO (Fig. 13c) as well as between sea ice in the Chukchi/Beaufort seas farther south and the AO (Fig. 13d). It should be noted that because of the constraints of the quantitative metrics of sea ice areal coverage (i.e., consistently near 100% sea ice concentration during winter for the Canada Basin and Chukchi/Beaufort seas; and consistently 0% sea ice concentration

during summer for the Bering Sea), we would not expect to see significant correlation coefficients in these regions during those seasons, which we do not.

Ancillary datasets enable exploration of physical and biological components related to AMSR-E derived sea ice variability across the PAR, and include monthly SST data derived from the Aqua-MODIS sensor and monthly chlorophyll-*a* concentrations from the Globcolour Project. In particular, the months of June, July, and August, when sea ice retreats northward through the region and phytoplankton blooms are prevalent are most relevant to identifying biological shifts. The monthly mean sea ice concentrations, SST, and chlorophyll-*a* concentrations (over the AMSR-E record, 2003–2011) show a distinct seasonal transition as sea ice degrades, SST warms, and phytoplankton blooms occur throughout the region (Fig. 14). Chlorophyll-*a* concentrations are particularly high along the Bering Sea shelf break (i.e., the Bering Sea “Green

Belt”; Springer et al., 1996) and off Point Barrow during June, and in the western Bering Strait during all three months, which is consistent with areas of high nutrient upwelling. Apparent localized areas of high chlorophyll-*a* concentrations (within Norton Sound and at the mouths of the Mackenzie and Kolyma rivers) are likely artifacts of terrestrially derived organic matter and sediment and therefore not necessarily indicative of biological production. Theil-Sen median trends of monthly variables over the years 2003–2011 additionally give insights into related shifts across the region (Fig. 15). July trends in sea ice persistence indicate earlier breakup across the Beaufort Sea, whereas August trends in sea ice persistence indicate significant losses in both the Beaufort Sea and Canada Basin regions. Trends in SST show interesting patterns in the wake of sea ice shifts. For example, the Beaufort Sea (including the mouth of the Mackenzie River) shows warming trends in July and August as sea ice cover in that region has retreated

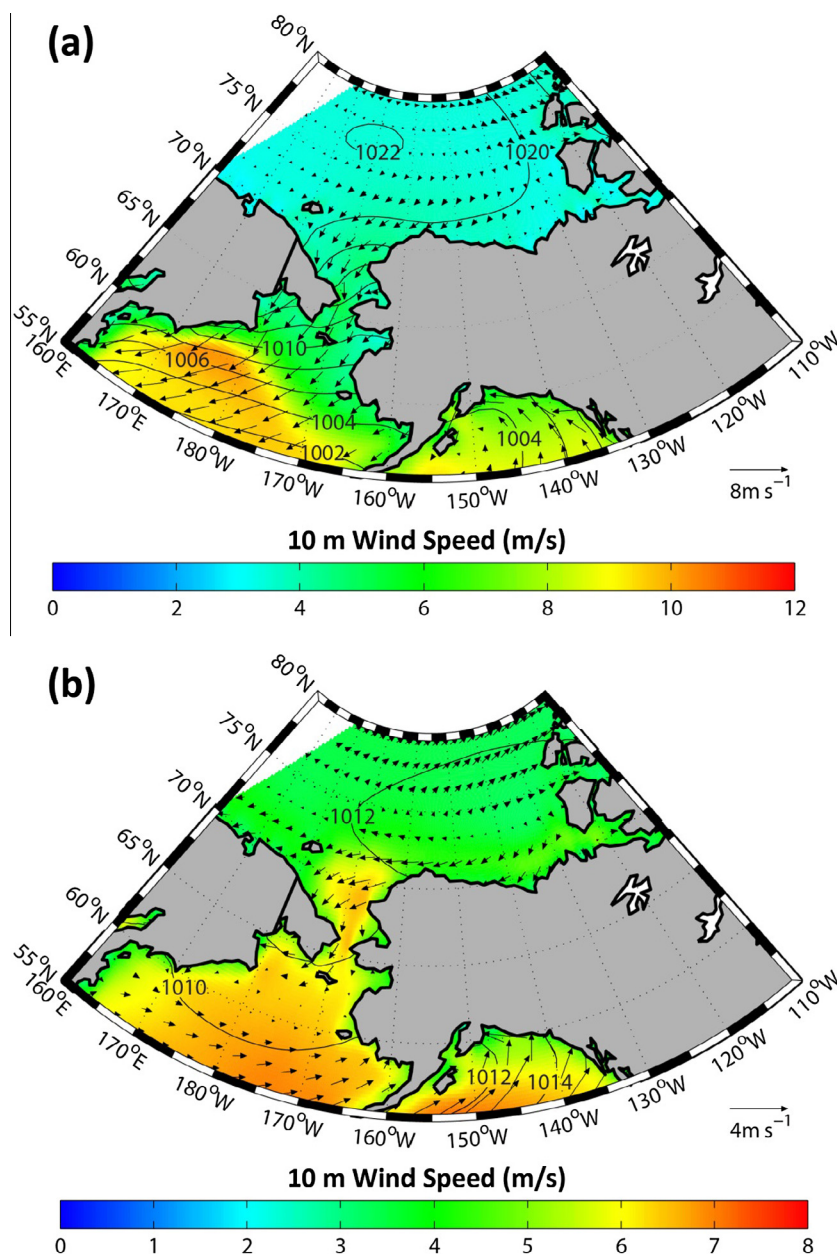


**Fig. 10.** Seasonal mean sea-level pressure (mb, contours), 10 m wind (m/s, vectors) and 10 m wind speed (m/s, color shading) during the (a) winter (JFM) and (b) summer (JAS) during the period 1979–2012.

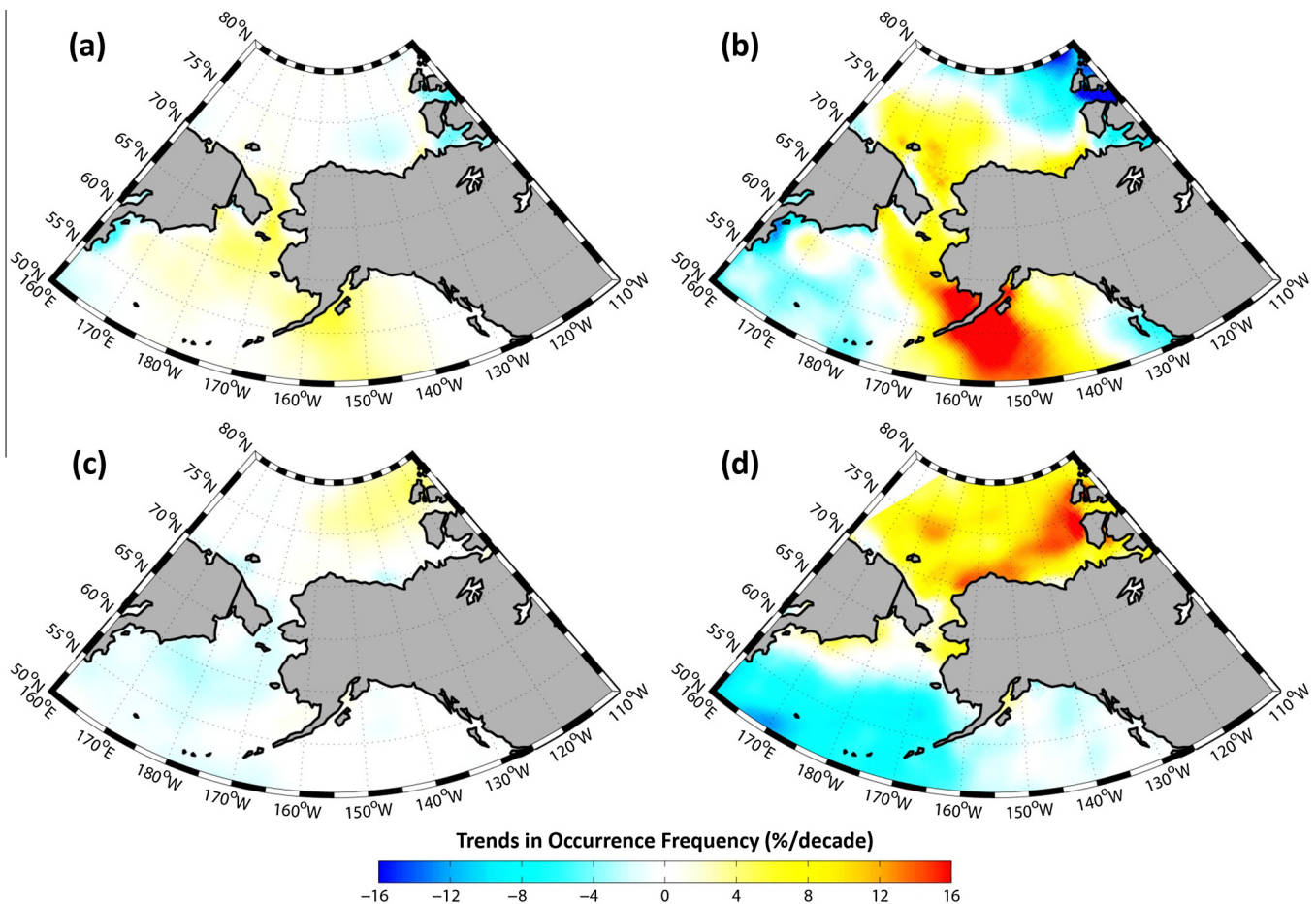


**Fig. 11.** Trends in the occurrence frequency (%/decade) of (a) winter (JFM) northwesterly 10 m winds during 1979–2012; (b) winter (JFM) northwesterly 10 m winds during 2000–2012; (c) summer (JAS) northeasterly 10 m winds during 1979–2012; and (d) summer (JAS) northeasterly 10 m winds during 2000–2012.

northward earlier each year and the Bering Sea shows cooling patterns in June, July, and August (after the winter/spring increases in sea ice cover). These cold ocean temperatures in the Bering Sea persisting in the wake of high sea ice years were additionally observed by [Stabeno et al. \(2012a\)](#), which they noted were also associated with relatively early phytoplankton blooms in March–April. Our findings here show that trends in chlorophyll-*a* concentrations are not spatially coherent, although areas worthy of note include increases along the Bering Sea shelf break and off Point Barrow in June, increases in the Chukchi Sea in July and August, and increases in the Beaufort Sea west of Banks Island in July and August.

#### 4. Discussion and conclusions

This study highlights recent variability in sea ice cover across the Bering, Chukchi, and Beaufort seas of the PAR, where trends in the loss of sea ice cover for the Chukchi and Beaufort seas have accelerated greatly over the past decade. In contrast, sea ice cover in the Bering Sea has exhibited multi-year patterns of variability over the satellite record, with notable gains in sea ice cover over the past decade. Winter gains in sea ice in the Bering Sea (up to ~9 days/year over the 2003–2011 period) are juxtaposed against summer losses in the Beaufort Sea (up to ~8 days/year) and north of the Chukchi Sea in the Canada Basin (up to ~7 days/year). [Comiso et al. \(2008\)](#) discussed similar acceleration of trends beginning in the late 1990s for the Arctic as a whole, although they did

not quantify this for specific sub-regions (nor had the Bering Sea yet shown such dramatic increases in sea ice cover as it has over this past decade). Sea ice variability can be instigated by multiple drivers, including cooling or warming air temperatures, changes in atmospheric circulation and ice motion, shifts in cloud cover, and advected ocean heat ([Perovich, 2011](#) and references therein). Wind speed and direction in particular have been identified as important drivers of sea ice edge variability ([Kimura and Wakatsuchi, 2001](#); [Rikiishi et al., 2005](#)). Preconditioning of the ice (e.g., [Nghiem et al., 2006](#); [Lindsay et al., 2009](#)) and ice-albedo feedbacks ([Perovich et al., 2007, 2008, 2011](#); [Perovich, 2011](#)) can set the stage for even more dramatic changes once shifts in sea ice are initiated. For example, earlier sea ice retreat allows for more solar radiation to be absorbed by ocean waters, resulting in seawater warming and a delay in sea ice formation the following autumn ([Stammerjohn et al., 2012](#)). This association between earlier sea ice breakup and later sea ice formation is observed in this study as well. While these feedbacks are clearly in play throughout the PAR, we observe in this study that the most rapid shifts in sea ice cover over the past decade in the Beaufort Sea have been primarily wind driven, those in the Canada Basin have been primarily thermally driven, and those in the Bering Sea have been influenced by elements of both.

Specifically, patterns of recent sea ice decline in the Beaufort Sea indicate that sea ice may be responding to enhanced northeasterly winds associated with a strengthened circulation throughout the region. This may have also impacted the activity of the Cape Bathurst polynya, which is proximal to the area of observed

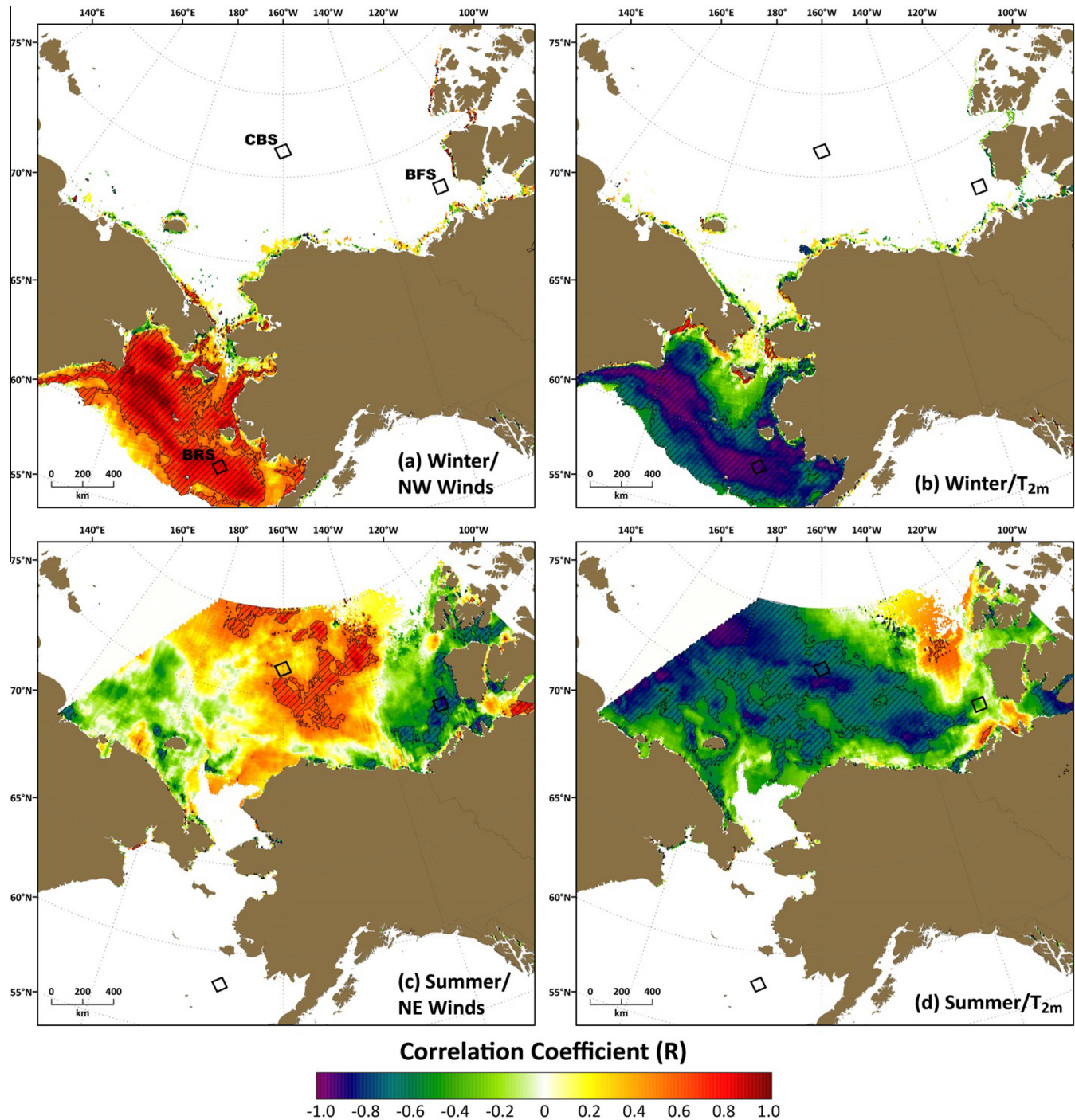


**Fig. 12.** Pearson correlation coefficients ( $R$ ) over the years 2003–2011 between sea ice persistence based on available AMSR-E sea ice concentrations (for the corresponding season) and the (a) occurrence frequency of winter (JFM) northwesterly 10 m winds; (b) winter (JFM) 2 m air temperature; (c) the occurrence frequency of summer (JAS) northeasterly 10 m winds; and (d) summer (JAS) 2 m air temperature. Hatching indicates statistically significant regions ( $p < 0.1$ ), where  $|R| \geq 0.582$ . Mean coefficients for representative sites CBS, BFS, and BRS are summarized in Table 2.

**Table 2**  
Pearson correlation coefficients for focused analysis sites in the Canada Basin (CBS), Beaufort Sea (BFS), and Bering Sea (BRS) over the years 2003–2011 between AMSR-E seasonal sea ice persistence (for the corresponding season) and the occurrence frequency of winter northwesterly 10 m winds and winter 2 m air temperature; as well as the occurrence frequency of summer (JAS) northeasterly 10 m winds and summer 2 m air temperature. Statistical significance of correlation coefficients is designated as  $p < 0.01$  (bolded/underlined) and  $p < 0.05$  (bolded).

	Winter (JFM)		Summer (JAS)	
	NW Winds	$T_{2m}$	NE Winds	$T_{2m}$
Canada Basin Site (CBS)	0	0	0.35	<b>-0.73</b>
Beaufort Sea Site (BFS)	0	0	<b>-0.77</b>	-0.29
Bering Sea Site (BRS)	<b>0.83</b>	<b>-0.91</b>	0	0

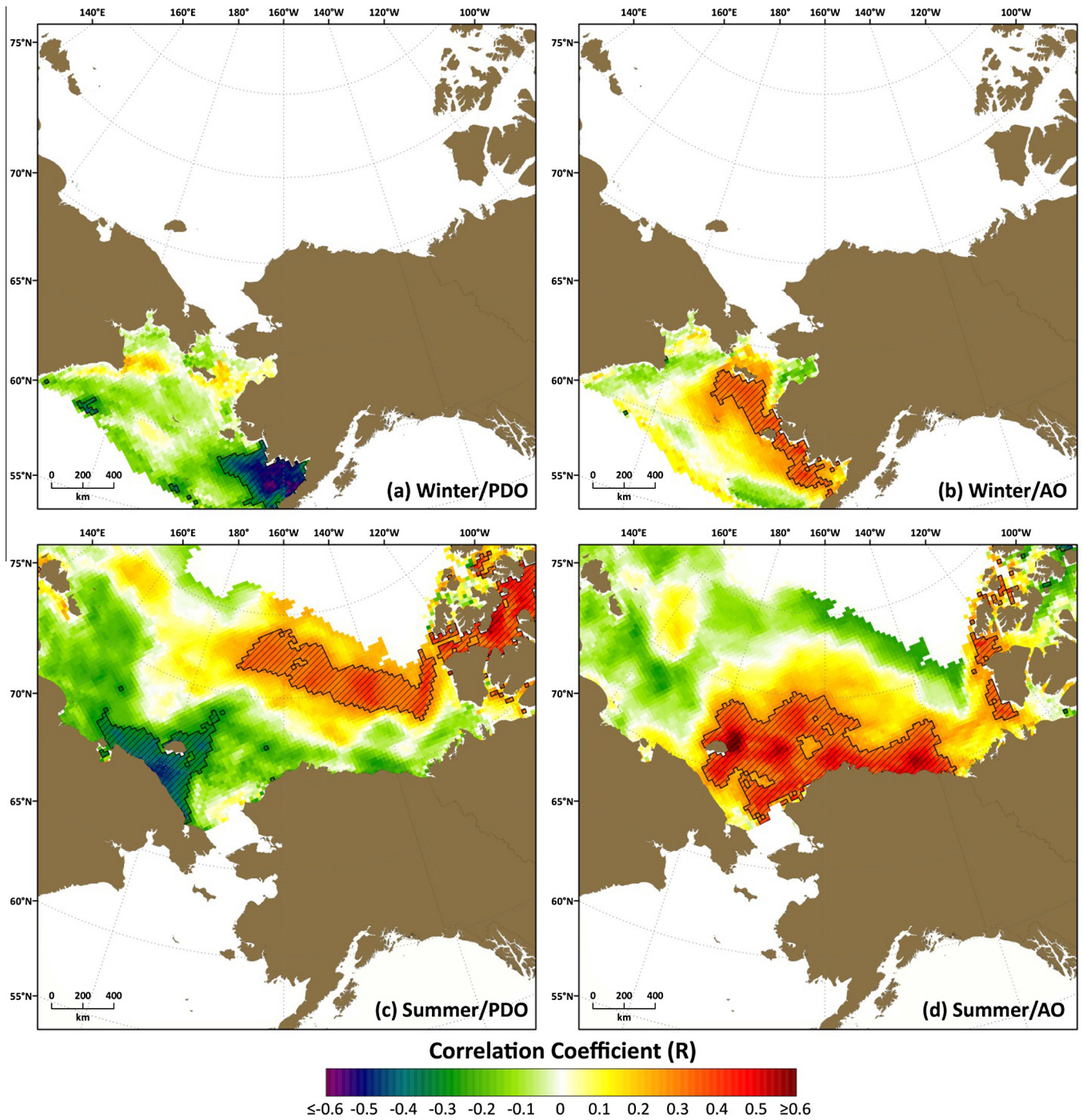


**Fig. 13.** Pearson correlation coefficients ( $R$ ) over the years 1979–2012 between sea ice persistence based on SMMR and SSM/I sea ice concentrations (for the corresponding season) and the (a) Pacific Decadal Oscillation (PDO) mean index during winter (JFM); (b) Arctic Oscillation (AO) mean index during winter (JFM); (c) PDO mean index during summer (JAS); and (d) AO mean index during summer (JAS). Hatching indicates statistically significant regions ( $p < 0.1$ ), where  $|R| \geq 0.287$ .

steepest sea ice declines in the Beaufort Sea near Banks Island. Indeed, Moore (2012) identified a trend toward a stronger Beaufort Sea High that began in the late 1990s, which is likely the result of tropospheric warming in the western Arctic and an associated reduction in atmospheric baroclinicity. A recent shift toward a more positive Arctic Dipole Anomaly since  $\sim 1995$  is also associated with a weakening Beaufort Gyre, enabling more ice to be flushed out of Arctic (Wu et al., 2006; Wang et al., 2009). The response of sea ice in the Beaufort Sea to these resulting enhanced northeasterly winds may have been preconditioned by an already thinner and weaker sea ice cover, which has been shown to

increase the responsiveness of ice drift to geostrophic winds (e.g., Kwok et al., 2013). Furthermore, these winds and their potential influence on the westward advection of warm waters associated with the Mackenzie River plume may also contribute to sea ice reductions in the eastern Beaufort Sea (e.g., Wood et al., 2015). We additionally observe that summer sea ice in the Chukchi Sea/Canada Basin region over the past decade has been positively correlated with these northeasterly winds, suggesting that sea ice blown out of the Beaufort Sea may be “piling up” in this region to the west. This effect may in fact be tempering trends of summer sea ice loss in the Chukchi Sea/Canada Basin that otherwise would

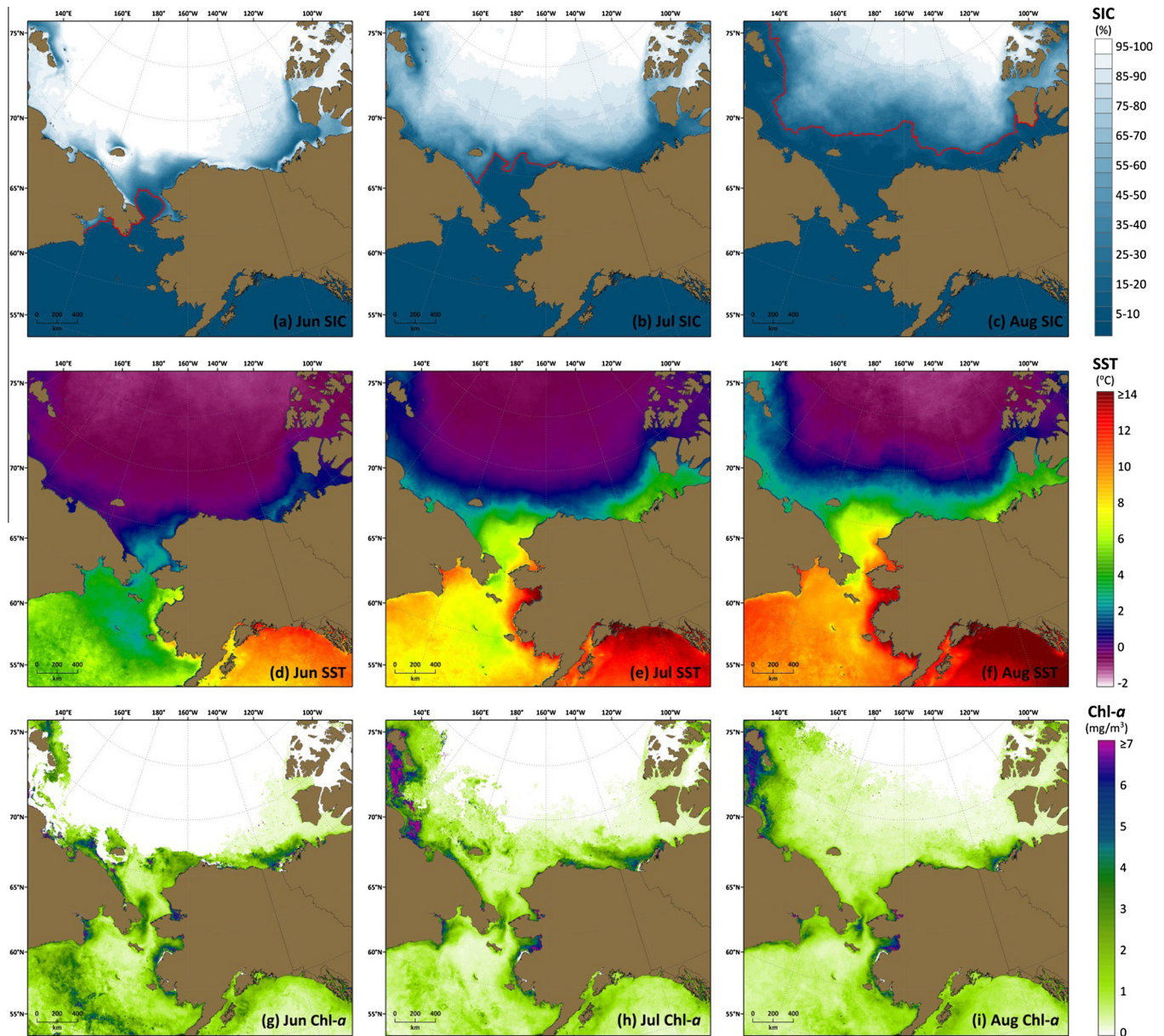


**Fig. 14.** Mean sea surface characteristics (2003–2011) through the sea ice breakup period for June, July, and August. AMSR-E mean sea ice concentration (SIC) for (a) June, (b) July, and (c) August where the red line indicates the mean sea ice edge (at 15% sea ice concentration) for each month; Aqua-MODIS mean sea surface temperature (SST) for (d) June, (e) July, and (f) August; and Globcolour mean surface chlorophyll-*a* (Chl-*a*) concentration for (g) June, (h) July, and (i) August.

have been even more extreme over the past decade. The potential displacement of ice from the Beaufort Sea westward is likely further enabled by the ongoing losses in the Chukchi Sea/Canada Basin region, which are shown here to be primarily thermally driven. We argue that these processes are part of a long-term secular trend related to broad-scale climate warming. In contrast to these long-term trends, we observe more complex multi-year variability in sea ice persistence in the Bering Sea where 1979–2000 was characterized by high interannual variability in sea ice, 2001–2005 was characterized by relatively low sea ice cover during a warm period, and 2006–2012 was characterized by relatively high sea ice cover during a cold period, which is similar to that also observed by Stabeno et al. (2012a). The recent increase in winter ice in the Bering Sea is likely a consequence of decadal weakening of the Aleutian Low (Overland et al., 1999; Rodionov et al., 2005), which has enhanced northwesterly winds that stimulate ice formation, as well as allowed for intrusion of colder air masses into the Bering Sea from Siberia (e.g., Francis and Hunter, 2007; Wendler et al.,

2014). These observations are the basis for our conclusion that winter ice increases in the Bering Sea are consequences of both thermal and wind-driven processes.

Various modes of climate variability have also been utilized to describe changes in sea ice, such as the PDO (Zhang et al., 2010; Danielson et al., 2011; Wendler et al., 2014) and AO (Wang and Ikeda, 2000; Rigor et al., 2002; Liu et al., 2004; Stroeve et al., 2011). In this study, as we were interested here in the longer-term influence of modes of climate variability over the past few decades since the start of the satellite record in the late 1970s, we quantitatively investigated the influence of the PDO and AO in particular on sea ice variability across the Bering, Chukchi, and Beaufort seas of the PAR. The PDO has been implicated for the recently observed increases in sea ice across the Bering Sea (e.g., Wendler et al., 2014), where a shift from dominantly positive PDO values to more negative values over the last decade has been associated with cooler sea surface temperatures across the region. Indeed, we find that the southeastern Bering Sea shelf region,

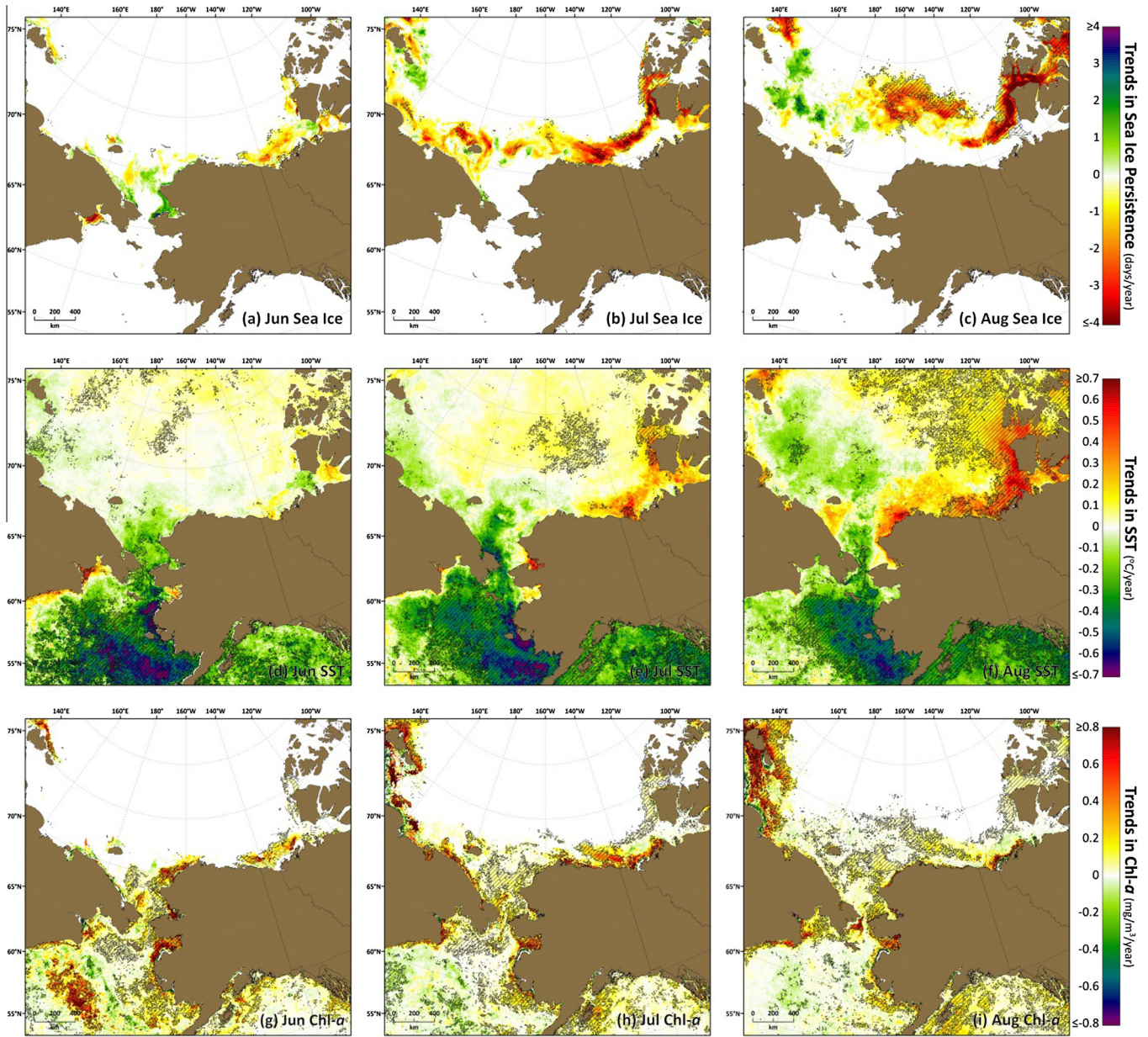


**Fig. 15.** Theil-Sen median trends in sea surface characteristics (over the years 2003–2011) through the sea ice breakup period for June, July, and August. Trends in AMSR-E derived monthly sea ice persistence during (a) June, (b) July, and (c) August; Aqua-MODIS derived SST during (d) June, (e) July, and (f) August; and Globcolour derived Chl- $a$  concentrations during (g) June, (h) July, and (i) August. Hatching indicates statistically significant regions ( $p < 0.1$ ) using the Mann–Kendall test for trend.

which has experienced the steepest gains in sea ice cover during winter over the past decade, is also associated with the most significantly negative correlations with the PDO (i.e., lower/negative PDO conditions associated with greater sea ice cover). The significant positive correlations observed between summer sea ice cover and the PDO (i.e., lower/negative PDO conditions associated with less sea ice cover) over the Canada Basin/Canadian Archipelago region is likely related to its connection with the Beaufort Sea High and associated pressure fields (Serreze and Barrett, 2011), where the recent intensification of the Beaufort Sea High (Moore, 2012) has likely contributed to reductions in sea ice throughout that region. During positive AO conditions, old and thick ice is flushed out of the Arctic and what remains is more prone to summer melting and also potentially wind-driven export; during negative AO conditions, winds and ice both flow clockwise across the Arctic which has typically retained more of the old, thick ice within

the Arctic region (Rigor et al., 2002). For the PAR specifically over the 1979–2012 time period, higher/positive AO conditions during winter are associated with more extensive ice in the Bering Sea south of St. Lawrence Island and higher/positive AO conditions during summer are associated with more extensive ice in the Chukchi and Beaufort seas. This more extensive summer ice in the Chukchi and Beaufort seas during higher/positive AO conditions may be a consequence of old and thick ice piling up here via winds that have pushed it out of the more central Arctic Ocean. However, over the last decade, these conditions appear to be shifting toward a new state. For example, Wang et al. (2009) suggested that since the AO has become mostly neutral or negative since 2002, there must now only be a weak link between the AO and the recently observed rapid ice retreat across the Arctic, and a new explanation for these recent record lows in sea ice must now exist (i.e., the Arctic Dipole Anomaly). Stroeve et al. (2011)

further explained that during recent negative AO years (such as the winter of 2009/2010), old and thick ice transported to the Beaufort and Chukchi seas did not survive the summer melt season. Thus, recent negative AO conditions (such as those over winter 2009/2010) that previously would have enhanced sea ice cover throughout the region may now be unable to counteract the present warmer climate, resulting in continued sea ice declines regardless of AO state.

Physical, biogeochemical, and biological consequences of these sea ice shifts are inevitable, where resulting impacts on ecosystem productivity across the PAR are particularly profound. Recent studies document significant increases in primary production in several sectors of the Arctic Ocean concomitant with sea ice declines. For example, satellite observations of primary production in the Arctic Ocean over a 12-year period (1998–2009) revealed a ~20% overall increase, resulting primarily from increases in open water extent (+27%) and duration of the open water season (+45 days) (Arrigo and van Dijken, 2011). Enhanced light availability through increasingly melt-ponded sea ice surfaces (Frey et al., 2011) is likely one of the key mechanisms that contributes to high levels of primary production underneath the ice (Arrigo et al., 2012, 2014). Although general increases in primary production are predicted to accompany continuing losses in sea ice cover, future shifts in primary production are expected to be spatially heterogeneous and dependent on several potentially confounding factors. For instance, modeling by Slagstad et al. (2011) suggests that while some Arctic shelves may have significant increases in primary production with further sea ice declines, the deep central basin of the Arctic Ocean may see (at most) small increases in production owing to low nutrient concentrations; areas that lose ice cover may see decreases in production owing to increased stratification with atmospheric warming (which is one factor controlling vertical nutrient distributions); and some inner coastal shelves may see little increase in production owing to the enhanced turbidity from river runoff and coastal erosion. The trends in chlorophyll biomass identified in this study are heterogeneous and not universally consistent with sea ice trends, which suggest that nutrient limitation (rather than simply sea ice/light limitation) is also a key factor controlling primary production. In summary, we suggest here that sea ice declines in the Chukchi Sea/Canada Basin and Beaufort Sea during summer are part of longer-term secular trends related to broad-scale climate warming, while recent increases in the Bering Sea during winter are part of multi-decadal variability in atmospheric circulation. As such, a synchronized shift toward annual declines in all three sub-regions may be a possibility in the near future and continued monitoring of sea ice variability across the PAR (and quantification of its various drivers) is of paramount importance for understanding how marine ecosystem productivity across all trophic levels may in turn respond.

## Acknowledgements

This study is part of the Synthesis of Arctic Research (SOAR) and was funded in part by the U.S. Department of the Interior, Bureau of Ocean Energy Management, Environmental Studies Program through Interagency Agreement No. M11PG00034 with the U.S. Department of Commerce, National Oceanic and Atmospheric Administration (NOAA), Office of Oceanic and Atmospheric Research (OAR), Pacific Marine Environmental Laboratory (PMEL). Additional funding was provided by the NASA Cryospheric Sciences Program (Grant NNX14AH61G to K. Frey, and Grant NNX10AH71G to K. Frey, L. Cooper, and J. M. Grebmeier) and the NSF Arctic Sciences Division (Grants ARC-0804773 and ARC-1107645 to K. Frey, and Grant ARC-1204082 to J. Grebmeier and L. Cooper). D. Mayer is thanked for assistance in sea ice

satellite data processing. G. W. K. Moore was supported by the Natural Sciences and Engineering Research Council of Canada.

## References

- Arrigo, K.R., van Dijken, G.L., 2011. Secular trends in Arctic Ocean net primary production. *Journal of Geophysical Research* 116, C09011. <http://dx.doi.org/10.1029/2011JC007151>.
- Arrigo, K.R., Perovich, D.K., Pickart, R.S., Brown, Z.W., van Dijken, G.L., Lowry, K.E., Mills, M.M., Palmer, M.A., Balch, W.M., Bahr, F., Bates, N.R., Benitez-Nelson, C., Bowler, B., Brownlee, E., Ehn, J.K., Frey, K.E., Garley, R., Laney, S.R., Lubelczyk, L., Mathis, J., Matsuoka, A., Mitchell, B.G., Moore, G.W.K., Ortega-Retuerta, E., Pal, S., Polashenski, C.M., Reynolds, R.A., Scheiber, B., Sosik, H.M., Stephens, M., Swift, J.H., 2012. Massive phytoplankton blooms under Arctic sea ice. *Science* 336, 1408. <http://dx.doi.org/10.1126/science.1215065>.
- Arrigo, K.R., Perovich, D.K., Pickart, R.S., Brown, Z.W., van Dijken, G.L., Lowry, K.E., Mills, M.M., Palmer, M.A., Balch, W.M., Bates, N.R., Benitez-Nelson, C.R., Brownlee, E., Frey, K.E., Laney, S.R., Mathis, J., Matsuoka, A., Mitchell, B.G., Moore, G.W.K., Reynolds, R.A., Sosik, H.M., Swift, J.H., 2014. Phytoplankton blooms beneath sea ice in the Chukchi Sea. *Deep Sea Research II*. <http://dx.doi.org/10.1016/j.dsr2.2014.03.018>.
- Barber, D.G., Hanesiak, J.M., 2004. Meteorological forcing of sea ice concentrations in the southern Beaufort Sea over the period 1979 to 2000. *Journal of Geophysical Research-Oceans* 109 (C6). <http://dx.doi.org/10.1029/2003JC002027>.
- Cavaliere, D.J., Parkinson, C.L., 2012. Arctic sea ice variability and trends, 1979–2010. *Cryosphere* 6 (4), 881–889. <http://dx.doi.org/10.5194/tc-6-881-2012>.
- Cavaliere, D., Parkinson, C., Gloersen, P., Zwally, H.J., 2008. *Sea Ice Concentrations from Nimbus-7 SMMR and DMSP SSM/I Passive Microwave Data*. National Snow and Ice Data Center. Digital media, Boulder, Colorado, USA.
- Comiso, J.C., Parkinson, C.L., Gertson, R., Stock, L., 2008. Accelerated decline in the Arctic sea ice cover. *Geophysical Research Letters* 35, L01703. <http://dx.doi.org/10.1029/2007GL031972>.
- Danielson, S., Curchitser, E., Hedstrom, K., Weingartner, T., Stabeno, P., 2011. On ocean and sea ice modes of variability in the Bering Seas. *Journal of Geophysical Research* 116, C12034. <http://dx.doi.org/10.1029/2011JC007389>.
- Francis, J.A., Hunter, E., 2007. Drivers of declining sea ice in the Arctic winter: a tale of two seas. *Geophysical Research Letters* 34 (17). <http://dx.doi.org/10.1029/2007gl030995>.
- Frey, K.E., Perovich, D.K., Light, B., 2011. The spatial distribution of solar radiation under a melting Arctic sea ice cover. *Geophysical Research Letters* 38, L22501. <http://dx.doi.org/10.1029/2011GL049421>.
- Grebmeier, J.M., 2012. Shifting patterns of life in the Pacific Arctic and sub-Arctic seas. *Annual Review of Marine Science* 4 (63–78). <http://dx.doi.org/10.1146/annurev-marine-120710-100926>.
- Hoaglin, D.C., Mosteller, F., Tukey, J.W., 2000. *Understanding Robust and Exploratory Data Analysis*, Wiley Classics, Wiley Classics Library ed. Wiley, New York.
- Holland, M.M., Bitz, C.M., Tremblay, B., 2006. Future abrupt reductions in the summer Arctic sea ice. *Geophysical Research Letters* 33, L23503. <http://dx.doi.org/10.1029/2006GL028024>.
- Hutchings, J.K., Rigor, I.G., 2012. Role of ice dynamics in anomalous ice conditions in the Beaufort Sea during 2006 and 2007. *Journal of Geophysical Research-Oceans* 117. <http://dx.doi.org/10.1029/2011JC007182>.
- Jin, M., Deal, C., Wang, J., McRoy, P., 2009. Responses of lower trophic level productivity to long-term climate changes in the southeastern Bering Sea, 1960–2007. *Journal of Geophysical Research* 114, C04010. <http://dx.doi.org/10.1029/2008JC005105>.
- Kendall, M.G., 1975. *Rank Correlation Methods*, fourth ed. Charles Griffin, London.
- Kimura, N., Wakatsuchi, M., 2001. Mechanisms for the variation of sea ice extent in the Northern Hemisphere. *Journal of Geophysical Research-Oceans* 106 (C12), 31319–31331. <http://dx.doi.org/10.1029/2000JC000739>.
- Kwok, R., Cunningham, G.F., 2012. Deformation of the Arctic Ocean ice cover after the 2007 record minimum in summer ice extent. *Cold Regions Science and Technology* 76–77, 17–23. <http://dx.doi.org/10.1016/j.coldregions.2011.04.003>.
- Kwok, R., Rothrock, D.A., 2009. Decline in Arctic sea ice thickness from submarine and ICESat records: 1958–2008. *Geophysical Research Letters* 36, L15501. <http://dx.doi.org/10.1029/2009GL039035>.
- Kwok, R., Cunningham, G.F., Wensnahan, M., Rigor, I., Zwally, H.J., Yi, D., 2009. Thinning and volume loss of the Arctic Ocean sea ice cover: 2003–2008. *Journal of Geophysical Research-Oceans* 114. <http://dx.doi.org/10.1029/2009JC005312>.
- Kwok, R., Spreen, G., Pang, S., 2013. Arctic sea ice circulation and drift speed: decadal trends and ocean currents. *Journal of Geophysical Research-Oceans* 118 (5), 2408–2425. <http://dx.doi.org/10.1002/jgrc.20191>.
- Laxon, S., Peacock, N., Smith, D., 2003. High interannual variability of sea ice thickness in the Arctic region. *Nature* 425, 947–950.
- Lindsay, R.W., Zhang, J., Schweiger, A.J., Steele, M.A., Stern, H., 2009. Arctic sea ice retreat in 2007 follows thinning trend. *Journal of Climate* 22, 165–176. <http://dx.doi.org/10.1175/2008JCLI2521.1>.
- Liu, J., Curry, J.A., Hu, Y., 2004. Recent Arctic Sea ice variability: connections to the Arctic Oscillation and the ENSO. *Geophysical Research Letters* 31, L09211. <http://dx.doi.org/10.1029/2004GL019858>.
- Mann, H.B., 1945. Non-parametric test against trend. *Econometrica* 13, 245–259.

- Markus, T., Stroeve, J.C., Miller, J., 2009. Recent changes in Arctic sea ice melt onset, freezeup, and melt season length. *Journal of Geophysical Research-Oceans* 114. <http://dx.doi.org/10.1029/2009jc005436>.
- Maslanik, J.A., Fowler, C., Stroeve, J., Drobot, S., Zwally, J., Yi, D., Emery, W., 2007. A younger, thinner Arctic ice cover: increased potential for rapid, extensive sea-ice loss. *Geophysical Research Letters* 34, L24501. <http://dx.doi.org/10.1029/2007GL032043>.
- Maslanik, J., Stroeve, J., Fowler, C., Emery, W., 2011. Distribution and trends in Arctic sea ice age through spring 2011. *Geophysical Research Letters* 38, L13502. <http://dx.doi.org/10.1029/2011GL047735>.
- Mesinger, F. et al., 2006. North American regional reanalysis. *Bulletin of the American Meteorological Society* 87, 343–360. <http://dx.doi.org/10.1175/BAMS-87-3-343>.
- Mizobata, K., Shimada, K., Saitoh, S., Wang, J., 2010. Estimation of heat flux through the eastern Bering Strait. *Journal of Oceanography* 66, 405–424. <http://dx.doi.org/10.1007/s10872-010-0035-7>.
- Moore, G.W.K., 2012. Decadal variability and a recent amplification of the summer Beaufort Sea High. *Geophysical Research Letters* 39. <http://dx.doi.org/10.1029/2012gl051570>.
- Nghiem, S.V., Chao, Y., Neumann, G., Li, P., Perovich, D.K., Street, T., Clemente-Colon, P., 2006. Depletion of perennial sea ice in the eastern Arctic Ocean. *Geophysical Research Letters* 33, L17501. <http://dx.doi.org/10.1029/2006GL027198>.
- Overland, J.E., Wang, M., 2013. When will the summer Arctic be nearly sea ice free? *Geophysical Research Letters* 40 (10), 2097–2101. <http://dx.doi.org/10.1002/grl.50316>.
- Overland, J.E., Adams, J.M., Bond, N.A., 1999. Decadal variability of the Aleutian Low and its relation to high-latitude circulation. *Journal of Climate* 12, 1542–1548.
- Overland, J.E., Francis, J.A., Hanna, E., Wang, M., 2012. The recent shift in early summer Arctic atmospheric circulation. *Geophysical Research Letters* 39 (19). <http://dx.doi.org/10.1029/2012GL053268>.
- Parkinson, C.L., Cavalieri, D.J., 2008. Arctic sea ice variability and trends, 1979–2006. *Journal of Geophysical Research-Oceans* 113 (C7). <http://dx.doi.org/10.1029/2007jc004558>.
- Perovich, D.K., 2011. The changing arctic sea ice cover. *Oceanography* 24 (3), 162–173.
- Perovich, D.K., Light, B., Eicken, H., Jones, K.F., Runciman, K., Nghiem, S.V., 2007. Increasing solar heating of the Arctic Ocean and adjacent seas, 1979–2005: attribution and role in the ice-albedo feedback. *Geophysical Research Letters* 34 (19). <http://dx.doi.org/10.1029/2007gl031480>.
- Perovich, D.K., Richter-Menge, J.A., Jones, K.F., Light, B., 2008. Sunlight, water, and ice: Extreme Arctic sea ice melt during the summer of 2007. *Geophysical Research Letters* 35, L11501. <http://dx.doi.org/10.1029/2008GL034007>.
- Perovich, D.K., Jones, K.F., Light, B., Eicken, H., Markus, T., Stroeve, J., Lindsay, R., 2011. Solar partitioning in a changing Arctic sea-ice cover. *Annals of Glaciology* 52 (57), 192–196.
- Polyakov, I. et al., 2007. Observational program tracks Arctic Ocean transition to a warmer state. *Eos, Transactions American Geophysical Union* 88 (40), 398. <http://dx.doi.org/10.1029/2007EO400002>.
- Rigor, I.G., Wallace, J.M., Colony, R.L., 2002. Response of sea ice to the Arctic Oscillation. *Journal of Climate* 15, 2648–2663.
- Rikiishi, K., Ohtake, H., Katagiri, Y., 2005. The role of atmospheric circulation in the growth of sea-ice extent in marginal seas around the Arctic Ocean. *Annals of Glaciology* 42, 352–360. <http://dx.doi.org/10.3189/172756405781813005>.
- Rodionov, S.N., Overland, J.E., Bond, N.A., 2005. The Aleutian low and winter climatic conditions in the Bering Sea. Part I: Classification. *Journal of Climate* 18, 160–177.
- Sen, P.K., 1968. Estimates of the regression coefficient based on Kendall's Tau. *Journal of American Statistical Association* 63, 1379–1389.
- Serreze, M.C., Barrett, A.P., 2011. Characteristics of the Beaufort Sea high. *Journal of Climate* 24, 159–182. <http://dx.doi.org/10.1175/2010JCLI3636.1>.
- Shimada, K., Kamoshida, T., Itoh, M., Nishino, S., Carmack, E., McLaughlin, F., Zimmermann, S., Proshutinsky, A., 2006. Pacific Ocean inflow: influence on catastrophic reduction of sea ice cover in the Arctic Ocean. *Geophysical Research Letters* 33, L08605. <http://dx.doi.org/10.1029/2005GL025624>.
- Slagstad, D., Ellingsen, I.H., Wassmann, P., 2011. Evaluating primary and secondary production in an Arctic Ocean void of summer sea ice: an experimental simulation approach. *Progress in Oceanography* 90, 117–131.
- Spreen, G., Kaleschke, L., Heygster, G., 2008. Sea ice remote sensing using AMSR-E 89 GHz channels. *Journal of Geophysical Research* 113, C02S03. <http://dx.doi.org/10.1029/2005JC003384>.
- Springer, A.M., McRoy, C.P., Flint, M.V., 1996. The Bering Sea Green Belt: shelf-edge processes and exosystem production. *Fisheries Oceanography* 5, 205–223.
- Stabeno, P.J., Kachel, N.B., Moore, S.E., Napp, J.M., Sigler, M., Yamaguchi, A., Zerbini, A.N., 2012a. Comparison of warm and cold years on the southeastern Bering Sea shelf and some implications for the ecosystem. *Deep-Sea Research II* 65–70, 31–45. <http://dx.doi.org/10.1016/j.dsr2.2012.02.020>.
- Stabeno, P.J., Farley Jr., E.V., Kachel, N.B., Moore, S., Mordy, C.W., Napp, J.M., Overland, J.E., Pinchuk, A.I., Sigler, M.F., 2012b. A comparison of the physics of the northern and southern shelves of the eastern Bering Sea and some implications for the ecosystem. *Deep-Sea Research II* 65–70, 14–30. <http://dx.doi.org/10.1016/j.dsr2.2012.02.019>.
- Stammerjohn, S., Massom, R., Rind, D., Martinson, D., 2012. Regions of rapid sea ice change: an inter-hemispheric seasonal comparison. *Geophysical Research Letters* 39, L06501. <http://dx.doi.org/10.1029/2012GL050874>.
- Steele, M., Ermold, W., Zhang, J., 2008. Arctic Ocean surface warming trends over the past 100 years. *Geophysical Research Letters* 35, L02614. <http://dx.doi.org/10.1029/2007GL031651>.
- Stroeve, J., Holland, M.M., Meier, W., Scambos, T., Serreze, M., 2007. Arctic sea ice decline: faster than forecast. *Geophysical Research Letters* 34, L09501. <http://dx.doi.org/10.1029/2007GL029703>.
- Stroeve, J., Serreze, M., Gearheard, S., Holland, M., Maslanik, J., Meier, W., Scambos, T., 2008. Arctic sea ice extent plummets in 2007. *Eos, Transactions American Geophysical Union* 89 (2), 13. <http://dx.doi.org/10.1029/2008EO020001>.
- Stroeve, J.C., Maslanik, J., Serreze, M.C., Rigor, I., Meier, W., Fowler, C., 2011. Sea ice response to an extreme negative phase of the Arctic Oscillation during winter 2009/2010. *Geophysical Research Letters* 38, L02502. <http://dx.doi.org/10.1029/2010GL045662>.
- Stroeve, J.C., Serreze, M.C., Holland, M.M., Kay, J.E., Maslanik, J., Barrett, A.P., 2012. The Arctic's rapidly shrinking sea ice cover: a research synthesis. *Climatic Change* 110, 1005–1027.
- Wang, J., Ikeda, M., 2000. Arctic oscillation and Arctic sea-ice oscillation. *Geophysical Research Letters* 27, 1287–1290.
- Wang, M., Overland, J.E., 2009. A sea ice free summer Arctic within 30 years? *Geophysical Research Letters* 36, L07502. <http://dx.doi.org/10.1029/2009GL037820>.
- Wang, M., Overland, J.E., 2012. A sea ice free summer Arctic within 30 years: an update from CMIP5 models. *Geophysical Research Letters* 39, L18501. <http://dx.doi.org/10.1029/2012GL0522868>.
- Wang, M., Overland, J.E., 2015. Projected future duration of the sea-ice-free season in the Alaskan Arctic. *Progress in Oceanography* 136, 50–59.
- Wang, J., Zhang, J., Watanabe, E., Ikeda, M., Mizobata, K., Walsh, J.E., Bai, X., Wu, B., 2009. Is the dipole anomaly a major driver to record lows in Arctic summer sea ice extent? *Geophysical Research Letters* 36, L05706. <http://dx.doi.org/10.1029/2008GL036706>.
- Wang, J., Eicken, J., Yu, Y., Bai, X., Zhang, J., Hu, H., Wang, D.-R., Ikeda, M., Mizobata, K., Overland, J.E., 2014. Abrupt climate changes and emerging ice-ocean processes in the Pacific Arctic Region and the Bering Sea. In: Grebmeier, J.M., Maslowski, W. (Eds.), *The Pacific Arctic Region: Ecosystem Status and Trends in a Rapidly Changing Environment*. Springer, Dordrecht, pp. 65–99.
- Wendler, G., Chen, L., Moore, B., 2014. Recent sea ice increase and temperature decrease in the Bering Sea area, Alaska. *Theoretical and Applied Climatology*. <http://dx.doi.org/10.1007/s00704-013-1014-x>.
- Wood, K.R., Overland, J.E., Salo, S.A., Bond, N.A., Williams, W.J., Dong, X., 2013. Is there a “new normal” climate in the Beaufort Sea? *Polar Research* 32, 19552. <http://dx.doi.org/10.3402/polar.v32i0.19552>.
- Wood, K.R., Bond, N.A., Overland, J.E., Salo, S.A., Stabeno, P., Whitefield, J., 2015. A decade of environmental change in the Pacific-Arctic region. *Progress in Oceanography* 136, 12–31.
- Woodgate, R.A., Aagaard, K., Weingartner, T.J., 2006. Interannual changes in the Bering Strait fluxes of volume, heat and freshwater between 1991 and 2004. *Geophysical Research Letters* 33, L15609. <http://dx.doi.org/10.1029/2006GL026931>.
- Wu, B., Wang, J., Walsh, J.E., 2006. Dipole anomaly in the winter Arctic atmosphere and its association with sea ice motion. *Journal of Climate* 19, 210–225. <http://dx.doi.org/10.1175/JCLI3619.1>.
- Yu, J., Liu, A.K., Yang, Y., Zhao, Y., 2013. Analysis of sea ice motion and deformation using AMSR-E data from 2005 to 2007. *International Journal of Remote Sensing* 34 (12), 4127–4141. <http://dx.doi.org/10.1080/01431161.2013.772314>.
- Zhang, J., 2005. Warming of the arctic ice-ocean system is faster than the global average since the 1960s. *Geophysical Research Letters* 32, L19602. <http://dx.doi.org/10.1029/2005GL024216>.
- Zhang, J., Woodgate, R., Moritz, R., 2010. Sea ice response to atmospheric and oceanic forcing in the Bering Sea. *Journal of Physical Oceanography* 40, 1729–1747. <http://dx.doi.org/10.1175/2010JPO4323.1>.